

INVESTIGATING HOT GAS IN THE HALOS OF TWO MASSIVE SPIRALS: OBSERVATIONS AND COSMOLOGICAL SIMULATIONS

JESPER RASMUSSEN,¹ JESPER SOMMER-LARSEN,² KRISTIAN PEDERSEN,² SUNE TOFT,³ ANDREW BENSON,⁴ RICHARD G. BOWER,⁵ AND LISBETH F. OLSEN²

Draft version February 18, 2018

ABSTRACT

Models of disk galaxy formation commonly predict the existence of an extended reservoir of hot gas surrounding massive spirals at low redshift. As a test of these models, we have obtained X-ray and optical data of the two massive edge-on spirals NGC 5746 and NGC 5170, in order to investigate the amount and origin of hot gas in their disks and halos. *Chandra* observations of NGC 5746 reveal evidence for diffuse X-ray emission with a total luminosity of $\sim 7 \times 10^{39}$ erg s⁻¹ surrounding this galaxy out to at least ~ 20 kpc from the disk, whereas an identical study of the less massive NGC 5170 fails to detect any extraplanar X-ray emission. Unlike the case for other disk galaxies with detected X-ray halos, the halo emission around NGC 5746 is not accompanied by extraplanar H α or radio emission, and there is no evidence for significant nuclear or starburst activity in the disk. In contrast to these other cases, the emission around NGC 5746 therefore appears to arise from the cooling of externally accreted material rather than from disk outflows. To verify this idea, we present results of cosmological simulations of galaxy formation and evolution, showing our observations to be in good agreement with expectations for cosmological accretion, while also confirming that the X-ray halos of other spirals do not fit well into an accretion scenario. We find that the estimated cooling rate of hot halo gas around NGC 5746 would provide sufficient material for star formation in the disk to proceed at its present rate. This lends support to the idea that a supply of hot ambient gas is potentially available as fuel for star formation in massive, nearby spirals, and suggests that accretion of hot gas could be important for maintaining the stellar disks of such galaxies. Finally, our results support the notion that hot halo gas constitutes most of the "missing" galactic baryons.

Subject headings: galaxies: formation — galaxies: haloes — galaxies: individual (NGC 5170, NGC 5746) — galaxies: ISM — galaxies: spiral — X-rays: galaxies

1. INTRODUCTION

Estimates of the cosmic baryon fraction, defined as the ratio of baryonic to total mass in the Universe, can be combined with constraints on the integrated mass function of galaxies to infer that most baryons in the Universe are in a hot, diffuse form at the present epoch (Balogh et al. 2001). Cosmological simulations suggest that 30–40 per cent of all baryons in the Universe reside in intergalactic filaments of shock-heated gas with temperatures $10^5 \lesssim T \lesssim 10^7$ K, the so-called warm/hot intergalactic medium, WHIM (e.g. Cen & Ostriker 1999; Davé et al. 2001). X-ray absorption studies have provided observational evidence for such a component along the line of sight towards a number of quasars (e.g. Tripp et al. 2000; Nicastro et al. 2005; Savage et al. 2005).

While most of the WHIM baryons are predicted to reside in structures of low overdensity, outside the dark matter halos of individual galaxies and groups of galaxies

(Davé et al. 2001), a potential repository for some of the "hidden" baryons in the Universe could be extended halos of hot ($\sim 10^6 - 10^7$ K) gas around individual galaxies, including spirals (e.g. Fukugita & Peebles 2006). Cosmological simulations suggest that the total mass of these "external" galactic baryons is comparable to that of stars and cold gas in the galaxies themselves (Sommer-Larsen 2006). In a cosmological context, observational support for such a scenario comes from the angular correlations between the galaxy distribution and the soft X-ray background, which indicate the presence of soft X-ray emission from WHIM surrounding individual galaxies (Soltan 2006).

The presence of extended hot gaseous halos around optically bright elliptical galaxies is well established from X-ray observations (e.g. O'Sullivan et al. 2001). The idea that also disk galaxies like the Milky Way could be embedded in such halos dates back to the pioneering work of Spitzer (1956) and is now integral to many semi-analytical models of disk galaxy formation (White & Rees 1978; White & Frenk 1991; Kauffmann et al. 1993; Somerville & Primack 1999; van Kampen et al. 1999; Cole et al. 2000; Hatton et al. 2003). In these models, galaxy dark matter halos are assumed to grow as predicted by spherical infall models, with gas accreting continuously along with the dark matter. During infall into the dark matter potential, the gas is heated, potentially to the halo virial temperature, subsequently cooling radiatively. If cooling is rapid, as is the case for characteristic gas temperatures

¹ School of Physics and Astronomy, University of Birmingham, Edgbaston, Birmingham B15 2TT, UK; jesper@star.sr.bham.ac.uk

² Dark Cosmology Centre, Niels Bohr Institute, University of Copenhagen, Juliane Maries Vej 30, DK-2100 Copenhagen, Denmark

³ European Southern Observatory, Karl-Schwarzschild-Str. 2, 85748, Garching bei München, Germany

⁴ Division of Physics, Mathematics, & Astronomy, California Institute of Technology, Mail Code 130-33, Pasadena, CA 91125, USA

⁵ Institute for Computational Cosmology, University of Durham, South Road, Durham DH1 3LE, UK

$T \lesssim 10^6$ K and hence relatively shallow potential wells, no accretion shock develops outside the evolving galactic disk. In these models, present-day spirals of total mass $M \lesssim 10^{11} M_\odot$ accrete gas which is predominantly in a cold, non-X-ray emitting phase at temperatures much lower than the virial temperature of their halo (Binney 1977; Birnboim & Dekel 2003; Binney 2004; Kereš et al. 2005). This ‘cold accretion’ mode would be particularly pronounced at high redshift, and would imply that most of the halo radiation is emitted as Ly α emission close to the disk. Indeed, observational support for this scenario is now appearing at both low and high redshift (see, e.g., van der Hulst & Sancisi 2004; Fraternali & Binney 2006; Nilsson et al. 2006 and references therein).

At higher galaxy masses and gas temperatures, the gas would emit at X-ray wavelengths but would cool less efficiently, and is then assumed in the models to flow in more slowly than in the fast-cooling regime. A hot X-ray emitting halo can develop, in which the infalling gas is eventually deposited where stopped by angular momentum (typically at a central distance of a few kpc). As in the ‘cold accretion’ mode, the gas may eventually condense to form stars in a rotationally supported disk. The accreting gas is not assumed to comprise an infinite, static reservoir, however; the quasi-static region is assumed in the models to be terminated by the accretion shock in the slow-cooling regime or at the galaxy itself in the fast-cooling regime.

This general picture has in recent years been backed by some hydrodynamical simulations of galaxy formation (Toft et al. 2002; Kereš et al. 2005), lending support to the general validity of the simplifying assumptions underlying semi-analytical models. For example, the cosmological simulations presented by Toft et al. (2002) showed the X-ray luminosity L_X of hot halo gas to scale strongly with disk circular velocity v_c (defined here as the rotation velocity at 2.2 times the disk scale-length; see Sommer-Larsen & Dolgov 2001 for details), with $L_X \propto v_c^{5-7}$, as also expected from semi-analytical models of galaxy formation. This clearly suggests that X-ray observations could provide a useful route to mapping out any material accreting onto massive spirals at the present epoch.

Extended X-ray halos have indeed been detected around numerous star-forming spirals (see Strickland et al. 2004; Tüllmann et al. 2006a; Tüllmann et al. 2006b and references therein; Li et al. 2006). However, these galaxies typically have at least moderately high star formation rates ($\gtrsim 1 M_\odot \text{ yr}^{-1}$), and in every single case so far, the detected halo X-ray emission coincides with extraplanar H α and radio continuum emission and can be associated with stellar feedback activity in the disk (Tüllmann et al. 2006a). Indeed, in many of these cases there is unambiguous kinematic evidence for outflows perpendicular to the disk (Strickland et al. 2004). Unlike the expectation for gravitationally heated gas, the X-ray luminosity of the gas in the halos of these galaxies is found to correlate with various measures of the disk star formation rate and with the energy input rate by supernovae (SN), but not with baryonic or H I mass in the disk. These works suggest the existence of a limiting star formation rate of $\approx 1 M_\odot \text{ yr}^{-1}$, below which such multi-phase gaseous halos are not generated (Tüllmann et al. 2006b). The

halos observed so far therefore seem to result as a consequence of stellar feedback in the disk rather than infalling intergalactic material.

While recent results indicate that ongoing cosmological accretion of gas is generally necessary to explain certain properties of spiral disks such as lopsidedness and warps (e.g. Bournaud et al. 2005; Shen & Sellwood 2006) and the presence of bars (Block et al. 2002; Bournaud & Combes 2002), the gas accretion history of spirals in general remains a poorly understood topic from an observational viewpoint. There is one case, however, the Milky Way itself, for which indirect arguments can be used to both ascertain the presence of a very extended hot gaseous halo (e.g. Moore & Davis 1994; Quilis & Moore 2001; Sembach et al. 2003) and constrain the infall rate of externally accreted gas (Rocha-Pinto & Maciel 1996; Pagel 1997; Casuso & Beckman 2004). Observations of the X-ray background also supports the idea that a reservoir of hot virial-temperature gas surrounds the Milky Way (e.g. Wolfire et al. 1995; Pietz et al. 1998; Kuntz & Snowden 2000). Despite this, it is neither clear whether any of the gas in this putative hot halo is actually cooling out to accrete onto the Milky Way disk, nor to what extent any infall of this gas balances that currently being removed from the disk by star formation, although some of the high-velocity H I clouds surrounding the Milky Way may represent condensed, accreting material.

Hence, with the possible exception of the Milky Way, extended, gaseous halos that can be unambiguously associated with cosmological accretion of gas onto spirals have yet to be detected (but see below). In a first study dedicated to directly detecting these halos through their X-ray emission, Benson et al. (2000) compared *ROSAT* observations of three massive, highly inclined spirals to predictions of simple cooling flow models. The failure of these authors to detect any hot gas around the galaxies translated into upper limits on the halo X-ray luminosity which, for their best-constrained case of NGC 2841, was found to be a factor of 30 below their model prediction. While their models were deliberately simplified versions of general semi-analytical ones, the result persists that both some simple analytical models and hydrodynamical simulations overpredict actual halo luminosities (Governato et al. 2004; Benson et al. 2000 and references therein), though the exact magnitude of this discrepancy has yet to be established.

More sensitive X-ray observations of carefully selected systems are required to settle the question of whether hot gas halos exist around quiescent spirals at all. This would be an important consistency check on the assumptions underlying existing disk galaxy formation models, and has become feasible with the current generation of X-ray telescopes, which boasts substantial improvements in sensitivity and spatial resolution compared to *ROSAT*. Motivated by this, we initiated a *Chandra* search for hot X-ray gas surrounding massive, quiescent disk galaxies. As part of this program, the discovery of hot halo gas around NGC 5746, with a total X-ray luminosity of $\sim 5 \times 10^{39} \text{ erg s}^{-1}$, was reported by Pedersen et al. (2006, hereafter Paper I). In the present paper, we elaborate on the presentation in Paper I, and describe our corresponding *Chandra* results for the less massive galaxy NGC 5170. The motivation underlying our target se-

lection is described in detail, as is the reduction and analysis of X-ray and H α data of both galaxies. The derived constraints on hot halo properties are also discussed in comparison to the X-ray halos seen around other galaxies, both late- and early-type. A comprehensive discussion of the origin and dynamical state of halo gas around NGC 5746 is then given. In order to facilitate a discussion within the framework of current theories of disk galaxy formation, we furthermore describe and present results from cosmological simulations of galaxy formation, comparing their predictions to the results for NGC 5746, NGC 5170, and other massive spirals. On this background, we discuss the implications for the gas accretion history of massive spirals and for models of disk galaxy formation and evolution.

This paper is structured as follows. In § 2 we outline our target selection, and in § 3 we detail the reduction and analysis of X-ray and optical data. Results for both galaxies are presented in § 4 and compared to those of other galaxies in § 5. The origin of hot halo gas around NGC 5746 is investigated in § 6, and comparisons are made to predictions of cosmological simulations in § 7. Our findings and conclusions are summarized in § 8. A Hubble constant of $H_0 = 75 \text{ km s}^{-1} \text{ Mpc}^{-1}$ is assumed throughout. The distances to NGC 5746 and NGC 5170 are then 29.4 and 24.0 Mpc, respectively (Tully 1988), with 1 arcmin corresponding to ~ 8.6 and ~ 7.0 kpc. Unless otherwise stated, all errors are reported at the 68 per cent confidence level.

2. TARGET SELECTION

The primary objective of this study is to map and characterize any diffuse X-ray gas surrounding isolated, quiescent disk galaxies. Our starting point was therefore the simulation results of Toft et al. (2002), in particular the result that halo X-ray luminosity L_X should scale strongly with disk circular velocity v_c . Hence, our target sample was drawn by searching the NED and Hyperleda databases for spiral galaxies with circular velocity $v_c \geq 280 \text{ km s}^{-1}$. According to the results of Toft et al. (2002), this would ensure that the target galaxies are massive enough to retain an X-ray halo detectable at the present day. The expected extraplanar X-ray luminosities of such galaxies would translate into a few hundred ACIS-I counts for galaxies within distances of a few tens of Mpc and for typical *Chandra* exposures of a few tens of ks. We consider this a reasonable lower limit for the detection of large-scale diffuse emission around nearby galaxies with *Chandra*. A further advantage of large v_c lies in the fact that the efficiency with which SN outflows can escape the disk and complicate the interpretation of our results is expected to decline with increasing disk mass.

In addition, we required our targets to meet the following criteria: i) inclination $i \geq 80^\circ$, enabling a clear view of any hot gas above the disk plane; ii) distance $D < 40$ Mpc, for sufficient angular extent on the sky to enable a discrimination between disk and halo gas, and to obtain a sufficiently strong X-ray signal; iii) Galactic latitude $|b| > 30^\circ$, to have a low column density of absorbing foreground Galactic hydrogen, given that any halo emission is expected to be fairly soft and thus subject to significant absorption by intervening material (this criterion excluded a galaxy like NGC 2613, recently studied

by Li et al. 2006); iv) the galaxies should be isolated (i.e. not be a member of a pair or a group/cluster) and show no significant signs of interaction, so as to include only undisturbed galaxies and avoid contamination from hot gas residing in an ambient intragroup/-cluster medium; v) in order to minimize contamination from outflows of hot gas, the galaxies should be quiescent, i.e. not show evidence for significant starburst activity or activity related to an active galactic nucleus (AGN). This excluded galaxies such as NGC 891, which displays extraplanar X-ray, H α , and radio emission associated with stellar feedback activity (see Temple et al. 2005 and references therein).

Imposing these strict criteria, only two galaxies remained, NGC 5746 and NGC 5170. We stress that, within our search criteria, our sample is only as complete as the galaxy catalogues included within NED and Hyperleda. We also note that our selection was not restricted to particular Hubble types, but given the $v_c \geq 280 \text{ km s}^{-1}$ criterion, the selection method is likely to bias against late-type spirals. Since such galaxies are likely to display higher star formation activity at present than early-type ones, this criterion is in turn likely to favor relatively quiescent spirals, as desired. Of our two galaxies, NGC 5746 is the most massive one, being an SBb spiral with a circular velocity $v_c = 318 \pm 10 \text{ km s}^{-1}$ (HyperLeda database). For our other target, the Sc spiral NGC 5170, updated values of v_c became available after we initiated this study, with v_c now estimated at the significantly lower value of $v_c = 247 \pm 3 \text{ km s}^{-1}$ (e.g. Kregel et al. 2004) rather than the value of $v_c = 296 \text{ km s}^{-1}$ (Tully 1988) assumed when selecting our targets. We adopt here this new value. Assuming $L_X \propto v_c^{5-7}$, this would imply a decrease in its predicted hot halo luminosity by a factor of 3–4 relative to our initial expectations. As we will see, this suggests that we should not expect the halo of this galaxy to be detectable in our *Chandra* data, a suggestion confirmed by our analysis. We can therefore effectively use the data of this galaxy as a consistency check of our analysis procedure for NGC 5746.

In terms of their star formation rate (SFR), both galaxies are fairly quiescent, as already evidenced by the fact that none of them is included in the revised catalog of bright *IRAS* galaxies (Sanders et al. 2003), despite their close proximity and large mass. Their 8–120 μm luminosities, based on *IRAS* fluxes from Moshir et al. (1990) for NGC 5746 and Rice et al. (1988) for NGC 5170, translate into global SFRs of 0.8 ± 0.2 (NGC 5746) and $0.3 \pm 0.1 \text{ M}_\odot \text{ yr}^{-1}$ (NGC 5170), using the relations of Sanders & Mirabel (1996) and Kennicutt (1998). This is equivalent to specific SFRs of $2.8 \pm 0.7 \times 10^{-4}$ (NGC 5746) and $1.3 \pm 0.4 \times 10^{-4} \text{ M}_\odot \text{ yr}^{-1} \text{ kpc}^{-2}$ (NGC 5170), assuming a circular disk of radius equal to the semi-major axis of D_{25} , the ellipse outlining a B -band isophotal level of 25 mag arcsec $^{-2}$. This could be compared to the value of $\sim 2 \text{ M}_\odot \text{ yr}^{-1}$, i.e. $\sim 3 \times 10^{-3} \text{ M}_\odot \text{ yr}^{-1} \text{ kpc}^{-2}$, for the moderately quiescent Milky-Way disk (see e.g. Casuso & Beckman 2004). From their *IRAS* 60 and 100 μm fluxes S_{60} and S_{100} , both galaxies furthermore display low far-infrared ‘temperatures’ of $S_{60}/S_{100} = 0.13 \pm 0.02$ (NGC 5746) and 0.28 ± 0.05 (NGC 5170), and ‘mass-normalized’ star formation rates L_{FIR}/L_B of 0.048 ± 0.012 and 0.037 ± 0.012 . These values are also indicative of low star formation activity (see e.g.

Read & Ponman 2001). Salient features of the observed galaxies are listed in Table 1.

3. OBSERVATIONS AND ANALYSIS

3.1. Data Preparation

Both disk galaxies were observed by *Chandra* (obs. ID 3928 and 3929) with the ACIS-I array as aimpoint and with the CCD's at a temperature of -120° C. Data were telemetered in Very Faint mode which allows for superior background suppression relative to standard Faint mode. To exploit this, the data were reprocessed and background screened using CIAO v3.3. Bad pixels were screened out using the bad pixel map provided by the reduction pipeline, and remaining events were grade filtered, excluding *ASCA* grades 1, 5, and 7. Periods of high background on the ACIS-I chips were filtered using 3σ clipping of the 0.3–12 keV lightcurves extracted in off-source regions in 200 s bins. Resulting lightcurves showed no flaring periods, leaving a total of 36.8 ks (NGC 5746) and 33.0 ks (NGC 5170) of cleaned exposure time. Blank-sky background data from the calibration database were screened and filtered as for source data, and reprojected to match the aspect solution of the latter. They were subsequently scaled to match our source data according to the 10–12 keV count rates (these deviated by an acceptable 5–6 per cent from the exposure ratio between source and background data).

An important issue for obtaining robust background estimates and singling out any halo X-ray emission is the ability to efficiently identify and remove point sources. This was a key limiting factor in the similar *ROSAT* study by Benson et al. (2000). The much narrower point spread function of *Chandra* allows us to easily excise point source regions without losing much detector area, thus preserving most of the available source and background counts. We identified point sources on the ACIS-I array using the wavelet-based CIAO tool *wavdetect*, adopting a threshold significance of 1.8×10^{-6} for each CCD, which should limit the number of spurious detections to ~ 1 per CCD. A total of 126 (NGC 5746) and 101 (NGC 5170) point sources were detected, in good agreement with the statistical expectation of ~ 25 background sources per CCD for a 35 ks pointing (cf. Summers et al. 2003). Inside D_{25} , we detect 20 and 17 sources, respectively. All point sources were masked out in the analysis of diffuse emission, using their 4σ detection ellipses from *wavdetect*.

3.2. X-ray and $H\alpha$ Imaging

To aid the search for any diffuse X-ray emission in and around the galactic disks, adaptively smoothed, background-subtracted, and exposure-corrected *Chandra* images of the central region around each galaxy were produced using a method similar to the one described by Rasmussen et al. (2006). Source images were first smoothed using the ASMOOTH algorithm (Ebeling et al. 2006) (based on the CSMOOTH procedure in CIAO), which employs a kernel size that adapts itself to achieve a certain signal-to-noise (S/N) level under the kernel. We adopted a significance interval of $3-5\sigma$, so that the local smoothing scale is increased until an S/N ratio of 3 is reached under the kernel, while features significant at more than 5σ are left unsmoothed. Background maps

were generated from blank-sky data and scaled to match the source count rates in source-free regions on the relevant chip. Using the map of adopted smoothing scales returned by the smoothing algorithm, the background images were then smoothed to the same spatial scales as the source data and subtracted from the latter. The resulting images were finally exposure-corrected using similarly smoothed, spectrally weighted exposure maps, with weights derived from spectral fits to the integrated diffuse emission. We stress that the resulting images served illustration purposes only and were not used for any quantitative analyses.

In addition to the X-ray data, we also obtained $H\alpha$ images of both galaxies with the Danish 1.54-m telescope at La Silla, Chile, for total exposures of 120 (NGC 5746) and 160 min (NGC 5170). In both cases, 20 min *R*-band images were also taken for subsequent continuum-subtraction. The frames were bias-subtracted, flat-fielded, and median-combined using standard IRAF procedures. Using the *R*-band image of each galaxy, we estimated and subtracted the continuum emission contribution to the $H\alpha$ image as follows. The two combined images were normalized to the same exposure time, and the *R*-band image was smoothed with a Gaussian kernel to match the broader point spread function of the $H\alpha$ image. The smoothed *R*-band image was then scaled to match the narrower width of the $H\alpha$ filter and subtracted from the $H\alpha$ image. For NGC 5746, the background in the resulting continuum-subtracted $H\alpha$ image had a large-scale gradient caused by stray light from a star just outside the field of view. We modeled this using the SExtractor software (Bertin & Arnouts 1996) with options set to save a full resolution interpolated background map. Parameters were optimized to generate a map sufficiently fine to represent large scale variations, and sufficiently coarse so as not to include local non-background structures (such as an $H\alpha$ halo around the galaxy). The resulting background map was then subtracted from the $H\alpha$ image.

3.3. X-ray Spectroscopy and Background Estimation

Given that any hot gaseous halo could cover a large fraction of the *Chandra* field-of-view in both cases, using our *Chandra* data for background estimation ('local' background subtraction) may not produce reliable results. Instead, the appropriate blank-sky background data from the calibration database were employed for background estimates, thus also taking advantage of the superior statistics of these background data. However, due to spatial variations in the soft X-ray background, the nominal *ROSAT* All-Sky Survey 0.5–0.9 keV fluxes at our two pointings are a factor ~ 1.5 (NGC 5746) and ~ 1.3 (NGC 5170) higher than the exposure-weighted mean value of the resulting blank-sky data. In order to account for this excess emission in spectral analysis, we adopted the commonly used 'double-subtraction' technique (e.g. Arnaud et al. 2002). We first extracted source spectra from which blank-sky data of the same detector region were then subtracted. The result includes any local soft X-ray background excess at our source pointings relative to the blank-sky data. We then also extracted spectra in off-source regions ($7'-8'$ annuli) from our data and subtracted the associated blank-sky spectra, the result reflecting the spectrum of this soft back-

TABLE 1
SALIENT FEATURES OF THE OBSERVED DISK GALAXIES

Name	D (Mpc)	RA (J2000)	Dec (J2000)	Hubble Type	M_B	D_{25} (arcmin)	i	v_c (km s $^{-1}$)	N_H (cm $^{-2}$)
NGC 5746	29.4	14 ^h 44 ^m 56 ^s .00	+01 $^{\circ}$ 57'17''1	SBb	-21.79	(6.92, 1.20)	84 $^{\circ}$	318 ± 10	3.3×10^{20}
NGC 5170	24.0	13 ^h 29 ^m 48 ^s .83	-17 $^{\circ}$ 57'59''4	Sc	-21.18	(8.32, 1.20)	90 $^{\circ}$	247 ± 3	7.3×10^{20}

NOTE. — Distances taken from Tully (1988) (assuming $H_0 = 75$ km s $^{-1}$ Mpc $^{-1}$) and positions from the NASA/IPAC Extragalactic Database (NED). Absolute B magnitude, D_{25} (major and minor diameter), inclination i , and disk circular velocity v_c were taken from the Hyperleda database. Absorbing column density N_H is the Galactic value from Stark et al. (1992).

ground excess at our source pointings. These residual spectra were finally also subtracted from the blank-sky subtracted source-region spectra. Spectrally weighted response files were generated for the appropriate detector regions using CIAO.

An implication of the results described in the following section is that there could be residual source flux at the 20 per cent level in the 7'–8' annulus used for estimating the local background excess relative to the blank-sky data in the spectral analysis of NGC 5746. Since this local excess constitutes roughly half of the estimated total 0.3–2 keV background for NGC 5746, we could be underestimating the flux of the background-subtracted source spectrum by about 10 per cent in this band. However, vignetting differences between the source region and this annulus almost exactly compensates for this effect in terms of the total 0.3–2 keV flux, yielding a soft-band source flux which should be accurate to within 5 per cent in the spectral analysis. This is comparable to the statistical uncertainty on this quantity. Thus, though the distortions introduced to the total background spectrum by these competing effects should be small compared to the statistical uncertainty in each spectral bin, we have added a 20 per cent systematic error in quadrature to the statistical errors on all parameters obtained from spectral fitting of the NGC 5746 data.

For the spectral model fitting, a standard approach is to accumulate the spectra in bins of at least 20 net counts, and perform the fits assuming χ^2 statistics. However, since the diffuse emission in either galaxy is rather faint, we opted for a different approach in an attempt to maximally exploit the limited spectral information available. Instead, spectra were accumulated in bins of at least 5 net counts and fitted using Cash statistics. Since the Cash statistic does not provide a straightforward measure of the goodness of fit, we tested the quality of each fit by evaluating the corresponding reduced χ^2 statistic for the data binned into 20 cts bin $^{-1}$. This allowed us to readily reject models that were not statistically acceptable. As a second test, we confirmed that all fit results obtained in this way were consistent with those of the “standard” method. All fits were performed in the 0.3–5 keV band using XSPEC v11.3, assuming the Solar abundance table of Anders & Grevesse (1989).

4. RESULTS

4.1. X-ray and H α Images

Unprocessed *Chandra* images of each galaxy do not show any clear evidence for diffuse emission outside the disk regions. Adaptively smoothed 0.3–2 keV images, generated as described in § 2, are shown in Figure 1,

along with the optical extent (D_{25}) of the galaxies (note that a different version of the NGC 5746 image was shown in Paper I, in which each point source region prior to smoothing had been refilled by a Poisson distribution interpolated from a surrounding region using the CIAO task `dmfilth`). Although the resulting images should be interpreted cautiously, particularly given the fairly low X-ray surface brightness outside the disk of both galaxies, the smoothed images do display evidence for diffuse emission in the disks of both galaxies, with an indication that for NGC 5746 this emission extends well beyond the disk midplane. This is perhaps more easily seen in the center panel of Figure 1, which shows our reduced H α images of the two galaxies with the X-ray contours overlayed. Finally, in order to further enable a comparison to the radio continuum morphologies of the galaxies, the right panel shows again the H α data, this time with NRAO VLA Sky Survey 1.4 GHz data overlayed (Condon et al. 1998). This panel also displays the extraction regions discussed in the text below.

As can be seen, there is no significant evidence for diffuse H α or radio continuum emission extending well outside the optical disk of either galaxy. The two radio sources seen outside the optical disk of NGC 5746 are most probably background sources. They are not detected in our X-ray data despite the proximity of the galaxy, nor at near-infrared (2MASS) or optical wavelengths, and their 1.4 GHz fluxes of 38.9 and 27.1 mJy are not included in the value listed for the NGC 5746 disk by Condon et al. (1998). Moreover, radio sources in star-forming galaxies are known to form a tight radio–far-infrared correlation, with a ratio of 60 μ m to 1.4 GHz flux of $\log(S_{60}/S_{1.4 \text{ GHz}}) \approx 2.15$ (Condon & Broderick 1986; Condon et al. 1991). Assuming the two sources to be associated with NGC 5746, this relation would suggest their combined 60 μ m output to exceed that of the entire galaxy (1.3 ± 0.1 Jy; Moshir et al. 1990) by a factor of ~ 7 . This makes us conclude that these two sources are most likely associated with radio-loud background AGN.

A potential caveat associated with the interpretation of Fig. 1 is that the extraplanar emission apparent in this Figure could represent disk emission which has been smoothed beyond the disk by our adopted smoothing algorithm. Hence, in order to perform a more quantitative search for diffuse X-ray emission in and around the galaxies, and confirm the overall impression conveyed by Fig. 1, we generated 0.3–2 keV surface brightness profiles of the unsmoothed, exposure-corrected emission. The profiles were extracted perpendicular to the disks, within the rectangular regions labelled ‘A’ in Fig. 1, and with point sources masked out. Results are shown in Figure 2.

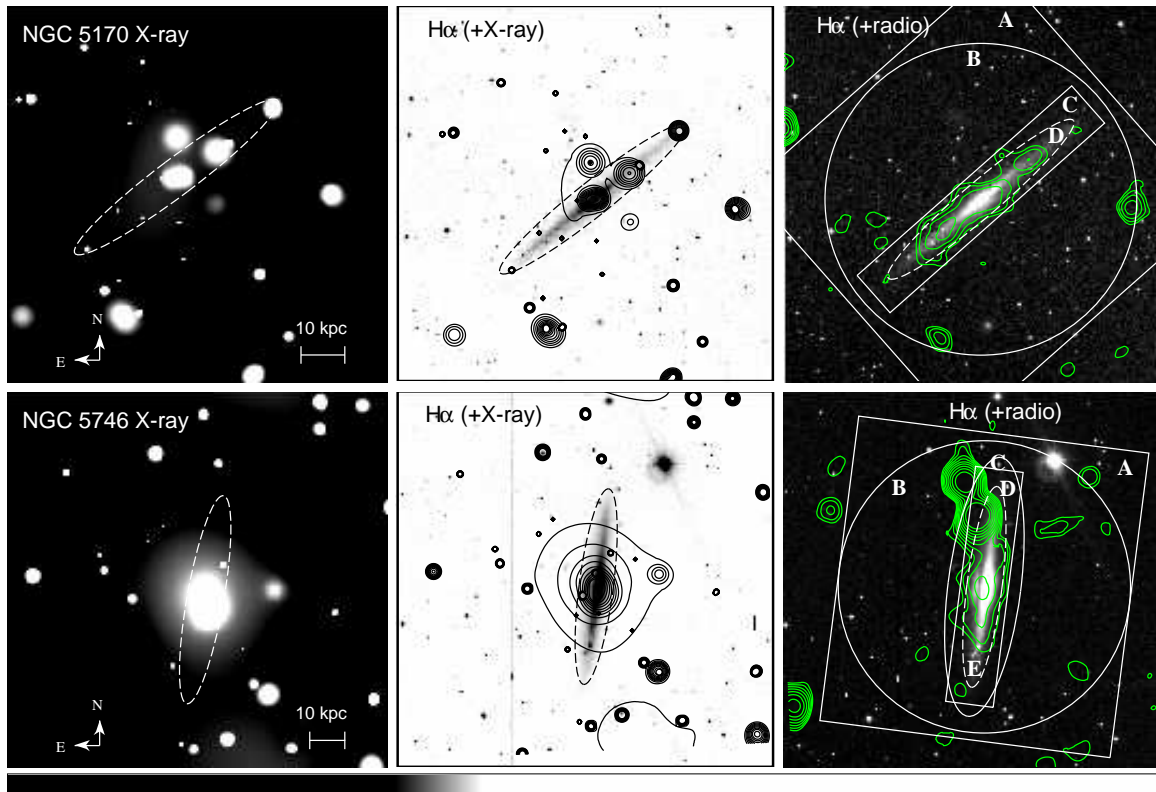


FIG. 1.— Left: Adaptively smoothed 0.3–2.0 keV *Chandra* images of the central 13×13 arcmin region around each galaxy. The images have been background-subtracted and exposure-corrected. Center: $H\alpha$ images with X-ray contours from the left figure overlaid. Contours are logarithmically spaced over a decade, beginning at 6.5×10^{-8} photons $\text{cm}^{-2} \text{s}^{-1} \text{arcmin}^{-2}$ for both galaxies. Right: $H\alpha$ images with NVSS 1.4 GHz contours, beginning at 1 mJy beam^{-1} and spaced by a factor of $\sqrt{2}$. Also shown are the regions used for extraction of X-ray surface brightness profiles ('A') and spectra (remaining regions). The innermost elliptical region shown in all figures outlines the D_{25} ellipse.

For NGC 5746, the individual surface brightness profiles on either side of the disk are seen to be mutually consistent within the errors. The figure also shows the profiles of both galaxies with the signal on both sides of the disk of each galaxy co-added to improve statistics. The corresponding profiles extracted from the exposure-corrected blank-sky background data within identical apertures are shown as dotted error bars. These provide an indication of the importance of CCD background variations and remaining instrumental signatures within the regions examined, allowing a test of whether the observed profiles can be explained by such effects.

Even if assuming no *a priori* knowledge of the background level in our two *Chandra* observations, Fig. 2 gives a clear indication of the presence of net excess emission outside the optical extent of NGC 5746. The result shown in Fig. 2 strongly suggests that the extended extraplanar emission evident in Fig. 1 is not an artefact of the smoothing procedure adopted when generating the X-ray image; excess emission is extending out to at least ~ 20 kpc on either side of the disk, with surface brightness decreasing with vertical distance to the disk. The profile bears no resemblance to that of the background data, confirming that the observed signal is real and not caused by instrumental artefacts or details of our analysis. For NGC 5170, on the other hand, the emission outside D_{25} is everywhere consistent with a con-

stant level equal to the estimated mean background level, and its distribution seems to follow that of the blank-sky background. This result, obtained in an identical way to that of NGC 5746, again confirms that the emission seen around NGC 5746 is not a product of our analysis method, thus supporting also the results indicated by the multi-wavelength comparison in Fig. 1. The presence of excess emission around NGC 5746 and the lack of any around NGC 5170 is further corroborated by the results of spectral analyses, as described below.

We characterized the co-added surface brightness profile of NGC 5746 using a model comprising a power-law plus a spatially constant background, $S = S_0|z|^{-\Gamma} + B_0$. We find $S_0 = 0.21^{+0.07}_{-0.04} \times 10^{-6} \text{ cts s}^{-1} \text{arcsec}^{-2}$, $\Gamma = 0.68^{+0.42}_{-0.35}$, and $B_0 = 0.15^{+0.02}_{-0.04} \text{ cts s}^{-1} \text{arcsec}^{-2}$, with a reduced $\chi^2_\nu = 0.67$ for 3 degrees of freedom ν . The uncertainties on Γ are large, but we note that the best-fitting background level resulting from this approach is entirely consistent with the value $B'_0 \approx 0.168 \times 10^{-6} \text{ cts s}^{-1} \text{arcsec}^{-2}$ determined independently from our spectral 'double-subtraction' background analysis, shown as a dotted line in Fig. 2. If fixing B_0 at this value in the fit to the profile, Γ becomes significantly better constrained to $\Gamma = 1.0 \pm 0.1$, with $S_0 = 0.25^{+0.06}_{-0.05} \times 10^{-6} \text{ cts s}^{-1} \text{arcsec}^{-2}$. This fit result is shown as a dashed curve in Fig. 2.

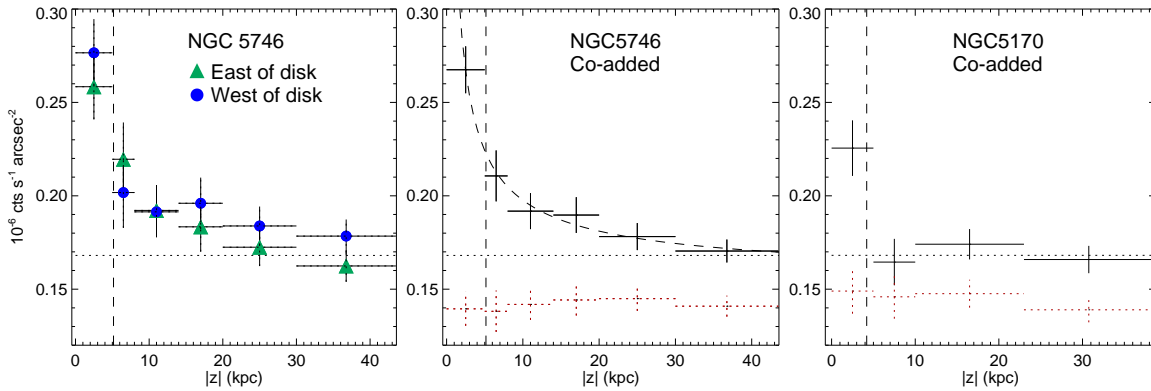


FIG. 2.— Surface brightness profiles of diffuse X-ray emission. The extent of D_{25} (minor axis) is marked by vertical dashed lines. Dotted data points show the level of the blank-sky background data prior to correction for excess soft X-ray background emission at our source pointings, while dotted horizontal lines represent the total mean background level estimated from ‘double-subtraction’ background spectra of the relevant regions, see § 3.3. For the NGC 5746 co-added profile, the dashed curve represents the best-fitting power-law model.

4.2. X-ray Spectra

For the extraction of spectra of the halo regions, the choice of aperture inner limit was a compromise between sampling regions close to the disk, where halo emission is expected to be strongly concentrated (Toft et al. 2002), and a need to remain insensitive to the presence of any outflowing gas from the disk resulting from, for example, star formation activity. However, given the low specific star formation rates of the disks (of order $10^{-4} \text{ M}_{\odot} \text{ yr}^{-1} \text{ kpc}^{-2}$, cf. § 2) one could *a priori* expect very little outflowing hot gas resulting from such activity. The investigation presented in § 6 below indicates that this assertion is justified. For both galaxies, many of the results presented below therefore apply to the region immediately outside D_{25} . Spectra obtained at larger distances from the disk produce consistent results but naturally return larger uncertainties on fitted parameters. For NGC 5746, the aperture outer limit was chosen with the guidance of Fig. 2, and with the general aim of maximizing the S/N ratio. For NGC 5170, with its smaller v_c and hence presumably lower halo L_X , we simply used regions whose physical extent are slightly smaller than those of NGC 5746.

Selected results for the different source regions labelled ‘B’–‘E’ in Fig. 1 are presented in Table 2. For NGC 5746, the background-subtracted spectrum underlying the bold-faced halo result listed in the Table is shown in Figure 3a. Excess 0.3–2 keV emission outside D_{25} is detected at 5σ . Its properties are well described by an optically thin thermal plasma (*mekal* model in XSPEC), with $T = 0.56^{+0.13}_{-0.18} \text{ keV}$. From the fractional 1σ errors on the normalization of this best-fitting spectral model, we derive a total unabsorbed 0.3–2 keV halo luminosity of NGC 5746 of $7.3 \pm 3.9 \times 10^{39} \text{ erg s}^{-1}$. The derived halo metallicity is low, $Z = 0.04^{+0.09}_{-0.02}$, but since statistics are too poor to constrain any temperature variations within the halo, we cannot exclude the possibility that the derived metallicity could be biased downwards due to the well-known Fe bias (arising when fitting a multi-temperature plasma with a single-temperature model; see Buote 2000). For the derived temperature, the halo luminosity remains within the quoted errors for all subsolar metallicities, however. We note that excess

emission at $> 4\sigma$ significance is found well outside the disk in our spectral analysis (e.g., region $B \setminus C$ in Table 2). This confirms, independently of the extracted surface brightness profile, that the extraplanar emission seen in Fig. 1 does not represent smoothed disk emission. For comparison, Figure 3b also shows a background-subtracted spectrum of the NGC 5746 *disk* emission. This is somewhat different from the halo spectrum, showing a tail at higher energies, possibly due to the presence of unresolved point sources in the disk.

For NGC 5170, no net emission is detected outside D_{25} , where the derived emission level remains consistent (at 1σ) with that of the background, as can be seen in Fig. 3c. An assumption about the halo temperature of this galaxy must therefore be made in order to constrain its L_X . To this end, we note that simulations predict a remarkably tight correlation between the temperature of infalling hot gas and v_c of the disk (Toft et al. 2002), with NGC 5746 falling onto this trend (see § 7). Hence, if assuming $T \approx 0.2 \text{ keV}$ for the hot halo of NGC 5170, as suggested by its disk circular velocity of $v_c \approx 250 \text{ km s}^{-1}$ (Toft et al. 2002) or by a simple expectation for the virial temperature $T_{\text{vir}} \approx (1/2)\mu m_p v_c^2$ of the underlying dark matter halo, we obtain an upper limit to its 0.3–2 keV luminosity of $L_X < 1.2 \times 10^{39} \text{ erg s}^{-1}$ for any subsolar metallicity. This upper limit is relaxed to $\sim 1.7 \times 10^{39} \text{ erg s}^{-1}$ if instead assuming, for example, $T \approx 0.15 \text{ keV}$, as would be appropriate for the significantly less massive Milky Way.

The disk emission of NGC 5746 cannot be described by a thermal component alone ($\chi^2_{\nu} = 4.38$ for 8 d.o.f.) but is well described by a thermal plasma of temperature $T \approx 0.3 \text{ keV}$ plus a power-law component, a result very similar to those obtained for the disks of other spirals, both quiescent galaxies and starbursts (e.g. Read et al. 1997; Rasmussen et al. 2004b and references therein). The thermal emission is most likely a signature of hot gas, shock heated by supernova explosions, whereas the power-law component may represent the integrated emission from a population of unresolved point sources, presumably mainly X-ray binaries and supernova remnants. Corrected for Galactic absorption and assuming $Z = Z_{\odot}$, the total 0.3–2 keV luminosity of the

TABLE 2
RESULTS OF SPECTRAL FITTING TO THE DIFFUSE X-RAY EMISSION

Region	Halo/ Disk?	Net Cts (0.3–2 keV)	S/N (0.3–2 keV)	XSPEC Model	Fit Results	χ^2/ν
<i>NGC 5746</i>						
B\E	H	230	5.1	<i>wabs(mekal)</i>	$T = 0.56^{+0.13}_{-0.18}$, $Z = 0.04^{+0.09}_{-0.02} Z_{\odot}$	9.77/9
				<i>wabs(pow)</i>	$\Gamma = 2.98^{+1.72}_{-1.75}$	10.99/9
B\D	H	192	4.8	<i>wabs(mekal)</i>	$T = 0.53^{+0.45}_{-0.25}$	5.53/8
B\C	H	175	4.4	<i>wabs(mekal)</i>	$T = 0.43^{+0.68}_{-0.24}$	5.83/7
E	D	122	10.6	<i>wabs(pow+mekal)</i>	$\Gamma = 0.44^{+0.40}_{-0.50}$, $T = 0.36^{+0.27}_{-0.18}$	4.28/6
(=D ₂₅)				<i>wabs(pow+2×mekal)</i>	$\Gamma = 0.43^{+0.42}_{-0.51}$, $T_1 = 0.13^{+25.5}_{-?}$, $T_2 = 0.71^{+6.84}_{-0.30}$	3.81/4
<i>NGC 5170</i>						
B\D	H	4	0.0
C	D	71	4.4	<i>wabs(pow)</i>	$\Gamma = 1.83^{+1.46}_{-1.00}$	3.75/4
				<i>wabs(mekal)</i>	$T = 8.75^{+?}_{-7.44}$	4.03/4
D	D	69	4.9	<i>wabs(pow)</i>	$\Gamma = 0.72^{+0.65}_{-0.57}$	2.87/3
(=D ₂₅)				<i>wabs(pow+mekal)</i>	$\Gamma = 0.21^{+0.63}_{-0.70}$, $T = 0.08^{+1.94}_{-?}$	0.28/1

NOTE. — Source regions are depicted in Fig. 1 ('B\D' means 'B excluding D'). Spectral model components are absorbed power-laws (intensity $\propto E^{-\Gamma}$) and thermal plasmas ("mekal"). The Galactic value of N_H (Table 1) is assumed for the absorbing component, with $Z = 0.1 Z_{\odot}$ and $Z = 1.0 Z_{\odot}$ for the halo and disk metallicities, respectively, where not specified otherwise. All temperatures are in keV. A '?' means that the uncertainty is unconstrained. Last column gives the goodness of fit for the number of degrees of freedom ν . Fit results for which $\chi^2_{\nu} > 2$ are not presented.

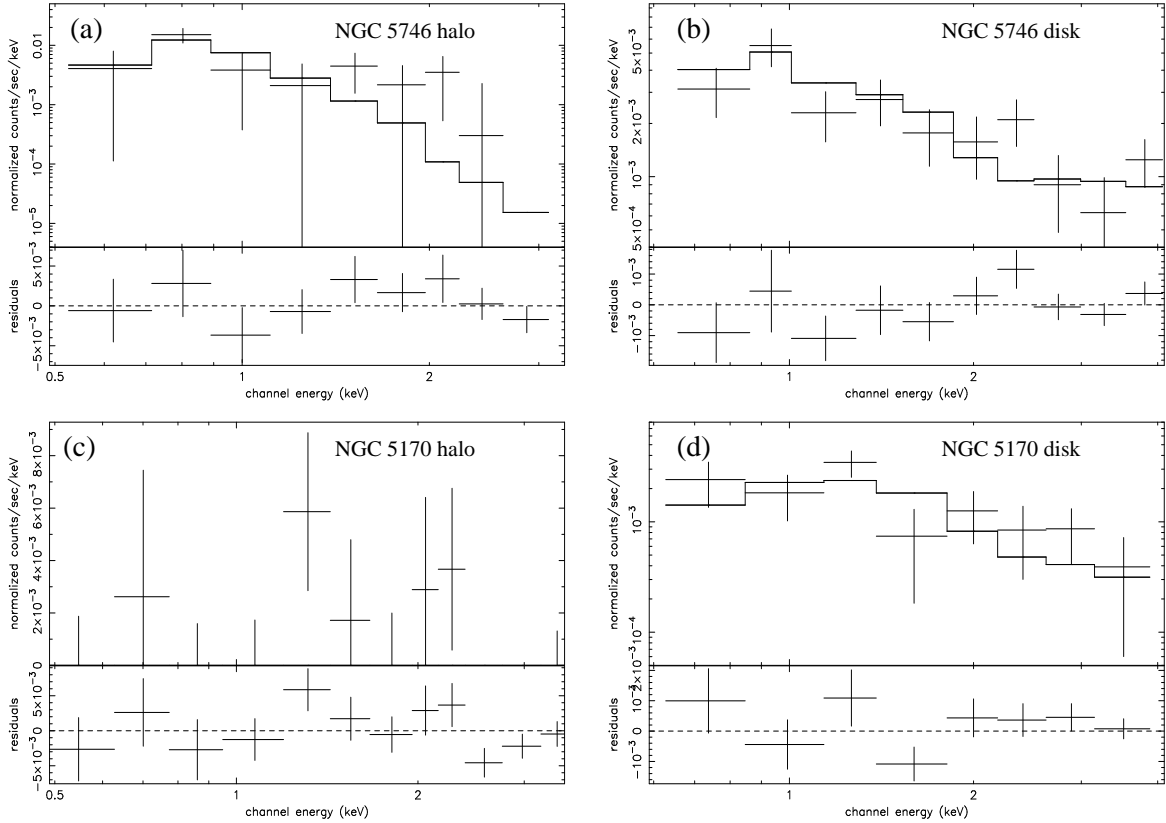


FIG. 3.— (a) Background-subtracted spectrum of NGC 5746 diffuse halo emission (region B\E of Table 2) along with the best-fitting thermal plasma model. Bottom panel shows fit residuals. (b) Corresponding plot for the NGC 5746 diffuse disk emission (region E of Table 2) along with the best-fitting thermal plasma + power-law model. (c) Spectrum of the NGC 5170 halo emission (region B\D of Table 2). Residuals show the deviation from zero net emission. (d) As (b), for the NGC 5170 disk emission (region D of Table 2).

NGC 5746 emission inside D_{25} is $\approx 3.7 \times 10^{39} \text{ erg s}^{-1}$, of which $1.2^{+0.6}_{-0.4} \times 10^{39} \text{ erg s}^{-1}$, i.e. $\sim 30 \pm 10$ per cent, is due to the power-law component. Some spiral disks show spectral evidence for a second thermal component, but while our data do not rule out this possibility for

the NGC 5746 disk, statistics are too poor to obtain useful constraints on such a model from spectral fitting (see Table 2).

For the same reason, the properties of the disk emission of NGC 5170 are not robustly characterized by our

data. A thermal model fit to the disk spectrum of this galaxy, shown in Fig. 3d, produces a physically absurd temperature of $T > 80$ keV, whereas a simple power-law provides an adequate description of the data. The reason could be strong intrinsic absorption in the disk, hardening the X-ray spectrum beyond that reproducible by a simple thermal model. A total unabsorbed 0.3–2 keV disk luminosity of $0.8^{+0.4}_{-0.3} \times 10^{39}$ erg s $^{-1}$ is derived for this galaxy.

5. PROPERTIES OF THE X-RAY GAS AND COMPARISON TO OTHER X-RAY HALOS

As we have seen, there is evidence from both imaging and spectra of diffuse X-ray emission surrounding NGC 5746 out to at least $|z| \sim 20$ kpc from the disk midplane. NGC 5170, on the other hand, does not display evidence of any detectable extraplanar X-ray emission. It is worth emphasizing that this notable difference between the two galaxies emerges after having subjected both data sets to the exact same data reduction and analysis procedure. This strongly suggests that the apparent surface brightness and spatial behaviour of the NGC 5746 extraplanar emission are genuine features, which cannot simply be ascribed to instrument characteristics, inaccurate background subtraction, or other details of our analysis method. Though a 5σ detection must be viewed as tentative rather than conclusive, we regard it as a sufficiently strong result to warrant a detailed discussion. The implications of a non-detection around NGC 5170 are also worth considering.

5.1. Properties of Halo and Disk Gas

Before discussing the properties of the detected emission in detail, we will briefly review whether the halo emission around NGC 5746 is truly diffuse or, given its low surface brightness, could potentially originate in a population of unresolved point sources. To test this, we repeated our source detection procedure using lower thresholds to see if sources just below the adopted threshold were present, but this was not found to be the case. Given the distribution of emission as a function of distance from the NGC 5746 disk (Fig. 2), any unresolved sources would have to be associated with NGC 5746 and so must on average have $L_X < 10^{38}$ erg s $^{-1}$ if assuming the halo spectrum of Fig. 3a. Although this is consistent with a population of X-ray binaries, the low emission level above $E \approx 2$ keV and the associated value of $\Gamma \sim 3$ for the best-fitting power-law do not fit well into this scenario. A significant contribution from either high-mass X-ray binaries or core-collapse supernova remnants is furthermore ruled out by the low galactic star formation rate. If the observed X-ray signal is, in turn, produced by low-mass X-ray binaries, these being tracers of stellar mass at an estimated level of $10^{10} M_\odot$ of stars per $\sim 8 \times 10^{38}$ erg s $^{-1}$ (Gilfanov 2004), the derived value of halo L_X would suggest the presence of several $10^{10} M_\odot$ of stars outside the disk region, another improbable scenario. This picture is made less probable still by the fact that a thermal plasma provides a marginally better spectral fit to the emission than a power-law model. In summary, the emission must be regarded as truly diffuse and is most probably due to a thermal plasma residing in an extended halo surrounding the galaxy.

Using the parameters derived for the NGC 5746 halo emission from the spectral analysis, the physical properties of the X-ray emitting halo gas can be assessed. From the spectral normalization A of the best-fit *mekal* model in XSPEC,

$$A = \frac{10^{-14}}{4\pi D^2} \int n_e n_H dV, \quad (1)$$

where D is the distance (Table 1), one can obtain the emission integral $EI \equiv \int n_e n_H dV \approx \eta n_e^2 V$ of the hot gas. Here η is the volume filling factor of the gas inside a total volume V ; we note that simulations (Toft et al. 2002; § 7) indicate high values of $\eta \approx 0.8$ –1, and that EI furthermore scales as Z^{-1} , where Z is the gas metallicity in solar units. We assume the large majority of detected X-ray gas to be confined inside a cylinder of height 2×20 kpc along the D_{25} minor axis (cf. Fig. 2) and a base radius of 45 kpc (Fig. 1). The volume of the disk is excluded, assuming this to be an ellipsoid of revolution with two identical major axes and a minor axis both equal to those of the D_{25} ellipse. This leaves a total volume $V = 6.9 \times 10^{69}$ cm 3 , which can be combined with the results for EI and the halo temperature $kT = 0.56^{+0.13}_{-0.18}$ keV, to derive various properties of the hot gas. Although these results will only be estimates and averages within the cylinder, we include here for completeness the formal statistical errors derived by propagating the errors on EI , T , and Z . For $\eta = 1$ we find a mean electron density $\langle n_e \rangle \sim (EI/V\eta)^{1/2} \approx 5.2^{+1.2}_{-1.7} \times 10^{-4}$ cm $^{-3}$, a gas mass $M_{\text{gas}} \sim m_p \langle n_e \rangle V \eta^{1/2} \approx 3.3 \pm 1.0 \times 10^9 M_\odot$, a mean cooling time $\langle t_{\text{cool}} \rangle \sim 3kT\eta^{1/2}/(\Lambda \langle n_e \rangle) \approx 1.4^{+0.7}_{-0.3} \times 10^{10}$ yr, and a corresponding gas cool-out rate $\langle \dot{M} \rangle \sim M_{\text{gas}}/\langle t_{\text{cool}} \rangle \approx 0.24 \pm 0.13 M_\odot \text{ yr}^{-1}$. Here we have used the cooling curves $\Lambda(T, Z)$ of Sutherland & Dopita (1993).

In the same approximation, the bulk properties of any halo gas around NGC 5170 can be constrained using similar arguments. Given the lack of halo detection, we must rely on simulation results for the gas temperature, and we take $T \approx 0.2$ keV as described earlier. Inside a volume derived the same way as for NGC 5746, and assuming $Z = 0.1 Z_\odot$, the derived upper limit to L_X can then be translated into corresponding limits to the gas parameters of $\langle n_e \rangle < 2.2 \times 10^{-4}$ cm $^{-3}$, $M_{\text{gas}} < 1.2 \times 10^9 M_\odot$, $\langle t_{\text{cool}} \rangle > 6.9 \times 10^9$ yr, and $\langle \dot{M} \rangle < 0.2 M_\odot \text{ yr}^{-1}$. Table 3 summarizes the derived constraints on halo properties for both galaxies.

For the X-ray gas in the disk of either galaxy, the filling factor and the intrinsic absorption remain largely unknown as they cannot easily be constrained from the present data. We will therefore refrain from attempting to constrain other quantities than the spectral properties of the disk gas already discussed in § 4.2. With the disks having far-infrared 40–120 μm luminosities of $L_{\text{FIR}} = 1.4 \times 10^{43}$ (NGC 5746) and 5.6×10^{42} erg s $^{-1}$ (NGC 5170), we note that their estimated diffuse X-ray luminosities render them consistent with the nominal L_X – L_{FIR} relation derived by Read & Ponman (2001) for the hot gas in ‘normal’ (i.e. non-starburst) spirals, $\log L_X \approx 1.1 \log L_{\text{FIR}} - 7.9$. As L_{FIR} is known to be a tracer of the star formation rate (e.g. Sanders & Mirabel 1996), these results provide further testimony to the modest star formation activity of both galaxies.

TABLE 3
DERIVED CONSTRAINTS ON HOT HALO GAS

Name	r (kpc)	T (keV)	Z (Z_{\odot})	L_X (erg s^{-1})	$\langle n_e \rangle$ (cm^{-3})	M_{gas} (M_{\odot})	$\langle t_{\text{cool}} \rangle$ (Gyr)	$\langle \dot{M} \rangle$ $M_{\odot} \text{ yr}^{-1}$
NGC 5746	43	$0.56^{+0.13}_{-0.18}$	$0.04^{+0.09}_{-0.02}$	$7.3 \pm 3.9 \times 10^{39}$	$5.2^{+1.2}_{-1.7} \times 10^{-4}$	$3.3 \pm 1.0 \times 10^9$	14^{+7}_{-3}	0.24 ± 0.13
NGC 5170	35	0.2 (fixed)	0.1 (fixed)	$< 1.2 \times 10^{39}$	$< 2.2 \times 10^{-4}$	$< 1.2 \times 10^9$	> 6.9	< 0.2

NOTE. — r is the outer radius of the aperture used for the extraction of mean halo properties. Luminosities are in the 0.3–2 keV band.

5.2. Comparison to Other Galactic X-ray Halos

In other cases where diffuse X-ray emission has been reported around spirals, this emission is typically accompanied by extended H α and radio halos, with a good correspondence between all three wavebands in terms of the extent and spatial structure of the extraplanar emission (e.g., Strickland et al. 2004; Tüllmann et al. 2006a). In particular, all existing studies that have reported the detection of extraplanar X-ray gas in ‘normal’ (moderately star-forming) spirals also present clear evidence of coincident extraplanar H α emission. To our knowledge, the only exception to this is NGC 2613 (Li et al. 2006), for which H α data do not appear to have been reported in the literature.

In these cases, the origin of these multi-phase halos have been linked to star formation activity in the disk (Wang et al. 2001, 2003; Ehle 2004; Strickland et al. 2004; Tüllmann et al. 2006a). It is well established that significant star formation activity in spirals is typically accompanied by the presence of diffuse ionized gas above the disk midplane, with temperatures of a few times 10^4 K (e.g. Rossa et al. 2004). The standard interpretation of the extraplanar X-ray, H α , and radio emission seen around other spirals is that the emission is indeed associated with multiple phases of gas, all expelled from the disk: The winds of supernovae and massive stars lift hot, X-ray emitting gas above the plane, along with warm and/or photoionized H α -emitting material, with the radio halo produced through synchrotron emission by SN-generated cosmic ray electrons which couple to the magnetic field of the outflowing gas (e.g. Wang et al. 2001, 2003).

Although there is no indication in Fig. 1 of significant extraplanar H α or radio emission around NGC 5746, we investigate this possibility in more detail in Fig. 4, where we show the surface brightness profile of the H α emission perpendicular to the disk. As can be seen, there is no evidence for significant amounts of H α gas outside the optical extent of the galaxy. Note that the dip in the H α profile 10 arcsec east of the D_{25} center is due to the dust lane also visible in Fig. 1. NGC 5170 has been studied in a similar way by Rossa & Dettmar (2000) who find no evidence for extraplanar diffuse H α emission surrounding this galaxy in an H α exposure of similar depth to ours. There is also no indication from Fig. 1 of significant extraplanar *radio* emission around either galaxy from VLA 1.4 GHz data, a conclusion supported for NGC 5746 by the VLA flux density profile also displayed in Fig. 4.

The absence of detectable extraplanar H α and radio emission in NGC 5746 is thus unique among spirals with X-ray halo emission. This suggests that the observed X-ray emission around NGC 5746 may have a different

origin than in the standard case where the emission can be linked to supernova-driven outflows. Another indication that this is the case can be based on comparing the X-ray luminosity of the extraplanar gas with the total (8 – 120 μm) infrared luminosity L_{IR} of the disk, adopting the standard assumption that the latter is a measure of the global disk star formation rate (see, e.g., Strickland et al. 2004). If the observed extraplanar X-ray emission around NGC 5746 were due to starburst winds driven by core-collapse SN, the ratio L_X/L_{IR} should then reflect the efficiency with which the mechanical energy output of SN in the disk is converted into thermal energy of extraplanar X-ray gas.

A comparison between extraplanar X-ray emission around other spirals, where detected, shows the ratio L_X/L_{IR} to be confined within a fairly narrow range, centered around a value which is in reasonable agreement with theoretical expectations for SN outflows (Strickland et al. 2004). The situation is illustrated in Figure 5, where we plot the infrared and extraplanar 0.3–2 keV luminosities for all disk galaxies for which – to our knowledge – X-ray halo emission has been reported. Included are the galaxies in the sample of Strickland et al. (2004), the additional galaxies of Tüllmann et al. (2006a), the recent result for NGC 2613 derived by Li et al. (2006), as well as those galaxies of Wang (2004) that are not included in the above samples. Where necessary, we have derived L_{IR} for these galaxies similarly to Strickland et al. (2004), using *IRAS* fluxes from Sanders et al. (2003) where available, and from Moshir et al. (1990) otherwise.

In contrast to these samples, as can be seen in the Figure, the value of L_X/L_{IR} derived for NGC 5746 is unusually high. The mean and 1σ dispersion of L_X/L_{IR} for the galaxies of Strickland et al. (2004) and Tüllmann et al. (2006a) is 0.68 ± 0.55 in the units displayed in Fig. 5, with the nominal value for NGC 5746 lying 13.6σ above this mean. It is worth pointing out that this difference arises, not because the halo L_X of NGC 5746 is conspicuously high, but because, as can be seen, its value of L_{IR} is unusually low for the derived extraplanar L_X . The immediate conclusion is that the NGC 5746 extraplanar emission seems to be of a different nature to that of the galaxies in the comparison sample.

How does the extraplanar emission of NGC 5746 compare to that seen in and around early-type galaxies? We note that the origin and heating mechanism of X-ray gas in elliptical galaxies remain controversial (e.g. O’Sullivan & Ponman 2004), and it is possible that different mechanisms are prevalent in low- and high-mass systems. Entering that debate is beyond the scope of this paper. A comparison is nonetheless warranted on the basis that the X-ray luminosity of diffuse gas in el-

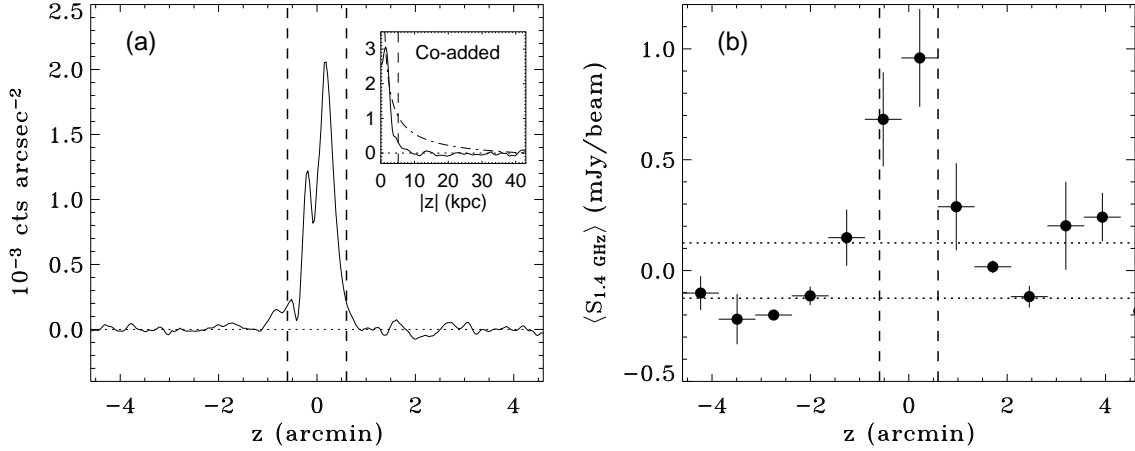


FIG. 4.— (a) Continuum-subtracted $H\alpha$ surface brightness profile of NGC 5746, extracted within the same aperture as that underlying Fig. 2. Bright stars have been masked out. Dashed vertical lines outline D_{25} as in Fig. 2, with the East side of the disk to the left. The inset shows the co-added $H\alpha$ profile (same units). The dot-dashed curve marks the best-fit power-law to the X-ray surface brightness, scaled to match the peak of the $H\alpha$ profile. (b) Corresponding mean flux density of 1.4 GHz continuum emission within the same aperture, in bins corresponding to the VLA beam size of 45 arcsec (FWHM). Bright point sources have been masked out. Dotted lines outline the 1σ errors on the noise level.

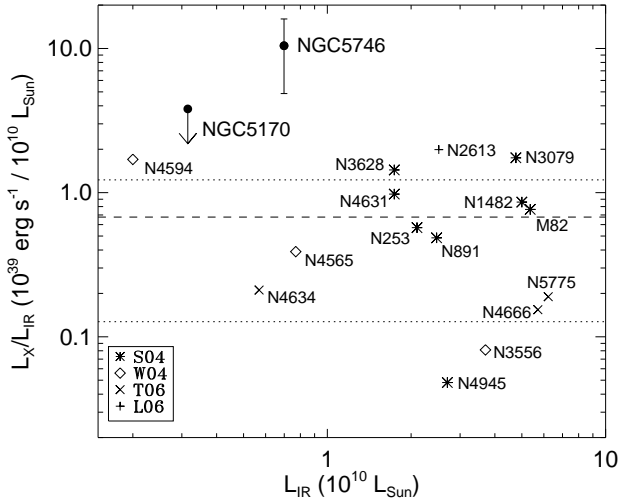


FIG. 5.— Infrared and extraplanar X-ray luminosities for NGC 5746, NGC 5170, and for the galaxies with detected extraplanar X-ray emission in the sample of Strickland et al. (2004, “S04”). Also shown are the corresponding results for the additional galaxies of Tüllmann et al. (2006a, “T06”), Wang (2004, “W04”), and Li et al. (2006, “L06”). Dashed and dotted lines show the mean and 1σ dispersion for the S04 + T06 galaxies.

ellipticals roughly obeys $L_X \propto L_B^2 \propto \sigma^{6-7}$ (based on the Faber-Jackson relation and the L_X – L_B relation of O’Sullivan et al. 2001), hence showing a similar dependence on the characteristic stellar velocity of the system to the one expected for the hot halos of spirals (§ 1). If similar processes are responsible for the emission around NGC 5746, one could perhaps expect this emission to follow similar scaling relations as those obeyed by E/S0’s.

The L_X – L_B and L_X – T relations derived for X-ray bright ellipticals by O’Sullivan et al. (2003) would nominally suggest $L_X \approx 2 \times 10^{41}$ and 1×10^{41} erg s $^{-1}$, re-

spectively, given L_B and (halo) T for NGC 5746. While these expectations lie well above the derived value for the NGC 5746 halo, both relations are subject to substantial scatter and can easily accommodate the NGC 5746 value. In addition, the agreement would improve if adding in the diffuse luminosity of the NGC 5746 disk, which would probably provide a more fair comparison (especially if also correcting this value for intrinsic absorption).

A comparison can also be made to the X-ray surface brightness profiles of ellipticals, which are typically found to be well described by standard β -models, with a mean value of $\beta \approx 0.55$ for X-ray luminous E’s (O’Sullivan et al. 2003), but again the scatter is substantial. For NGC 5746, the derived profile would correspond to $\beta \approx 0.35$, which would place it at the very low end of the range covered by these systems. On the other hand, it is clear that the profile derived for NGC 5746 must steepen beyond our radius of detection, as the total halo luminosity would otherwise diverge (this, of course, also applies to most of the ellipticals).

In summary, comparison to the diffuse emission of ellipticals is somewhat inconclusive and to a certain degree hampered by the fact that we are dealing with an edge-on galaxy, where (probably spatially varying) intrinsic absorption in the disk precludes a robust estimate of the *total* diffuse L_X . Taken at face value, the halo of NGC 5746 is less X-ray luminous for its disk L_B and halo T than the average X-ray bright elliptical, and also has a shallower surface brightness profile. However, the large scatter in the X-ray properties of ellipticals precludes a firm statement as to whether the diffuse X-ray emission around NGC 5746 is distinctively different from that seen in early-type galaxies.

6. ORIGIN OF NGC 5746 EXTRAPLANAR EMISSION

In Paper I it was briefly substantiated that the excess X-ray emission around NGC 5746 is most likely due to inflowing hot gas. Here we consider in detail possible alternatives, demonstrating that a hot gaseous halo of externally accreted gas indeed seems the most plausible

explanation for the origin of the detected extraplanar emission.

6.1. Gas Outflows from Stellar Activity

Given that NGC 5746 is isolated and hence should not be experiencing ram-pressure or tidal stripping of its hot disk gas, the most immediate explanation for its extraplanar X-ray emission would be outflows of hot gas powered by stellar activity in the disk. As already discussed, such outflows could be driven by core-collapse supernovae and mass loss from massive stars, or perhaps by SN Ia in the form of a bulge wind as suggested by Wang (2004). Although the limited X-ray signal does not allow us to entirely rule out this possibility, such a contribution seems unlikely to be significant for a number of reasons.

First of all, as mentioned, the hot halo properties of NGC 5746 are at variance with those of other spirals where the halo emission can be associated with SN outflows. In particular, Fig. 5 suggests that either mechanisms other than stellar processes are at work in generating the NGC 5746 halo, or, rather unlikely, the SN thermalization efficiency in the quiescent NGC 5746 is an order of magnitude higher than for the comparison sample shown in the figure, which includes actively star-forming spirals such as the prototypical starburst outflow galaxies M82 and NGC 253. The low metallicity derived for the halo gas also argues against a disk origin, although the robustness of this measurement can be questioned.

A second argument against stellar activity being responsible for the observed emission around NGC 5746 bases itself on the possibility of gas being blown out of the disk by SN activity. The large depth of the gravitational potential of NGC 5746 would be one factor which could inhibit stellar outflows from the disk. In practice, however, the distribution and pressure of the interstellar medium are usually more important factors for the possibility of blow-out than the depth of the gravitational potential (e.g. Mac Low & McCray 1988; Strickland & Stevens 2000). In a study of extraplanar X-ray emission detected around spiral galaxies covering a range of morphologies and star formation rates, Strickland et al. (2004) derived a criterion for gas blow-out based on the observed properties of the interstellar medium in typical spirals. They find on theoretical grounds that in order to have a collection of near-simultaneous SN expel gas out of the disk, the requirement $F_{\text{SN},\text{FIR},D_{25}} > 25 \text{ SN Myr}^{-1} \text{ kpc}^{-2}$ must be satisfied. In their notation, $F_{\text{SN},\text{FIR},D_{25}}$ is the rate $\mathcal{R}_{\text{SN}} = 0.2L_{\text{IR}}/10^{11} L_{\odot}$ of core-collapse SN per disk “area” D_{25}^2 , again assuming L_{IR} to be a proxy of the total star formation rate. Indeed, for the seven spirals in their sample with detected extraplanar X-ray emission, they find $F_{\text{SN},\text{FIR},D_{25}} > 40 \text{ SN Myr}^{-1} \text{ kpc}^{-2}$. By contrast, using an approach identical to that of Strickland et al. (2004), we obtain $L_{\text{IR}} = 7 \times 10^9 L_{\odot}$ and $F_{\text{SN},\text{FIR},D_{25}} \approx 4 \text{ SN Myr}^{-1} \text{ kpc}^{-2}$ for NGC 5746. Thus, the idea that star formation activity in NGC 5746 can blow out large quantities of gas to distances of $\sim 20 \text{ kpc}$ above the plane is in clear conflict with the results of Strickland et al. (2004). This result, of course, neglects the contribution from type Ia SNe, the rate of which may depend more sensitively on the total stellar mass than on the disk star formation rate. From the K - and B -band magnitudes of

NGC 5746, a type Ia SN rate of $\approx 0.01 \text{ yr}^{-1}$ can be estimated, using the prescription of Mannucci et al. (2005). This would imply $F_{\text{SN},\text{FIR},D_{25}} \approx 7 \text{ SN Myr}^{-1} \text{ kpc}^{-2}$ for the total SN rate (equivalent to 0.02 SN yr^{-1} over the full disk), still well below the criterion derived by Strickland et al. (2004).

Although the present level of stellar activity in the disk is thus unlikely to explain the X-ray emission around NGC 5746, the possibility remains that the gas was deposited in the halo by previous such activity. This would have had to happen sufficiently long ago to allow any $\text{H}\alpha$ and radio halo to fade away and return standard SFR indicators such as L_{FIR} of the disk to quiescent values. Indeed, it was argued in Paper I that the energy release required to set up the halo would involve the formation of $5\text{--}10 \times 10^9 M_{\odot}$ of stars, and that the age of such a hypothetical starburst would have to be at least 1–2 Gyr in order to comply with the present optical colours of NGC 5746. On the other hand, the derived hot gas properties translate into a *mean* cooling time at D_{25} of $t_{\text{cool}} = 3.9^{+2.0}_{-0.9} \times 10^9 \text{ yr}$. This sets a natural upper limit on the age of such a starburst.

From the observed correlation between far-infrared disk luminosity and the X-ray extent of a hot halo generated by an active starburst (Grimes et al. 2005), one would expect a characteristic extent of the extraplanar X-ray emission around NGC 5746 of only 1–2 kpc. This is in itself an argument against *ongoing* star formation activity being responsible for the NGC 5746 halo. If deposited in the halo by a starburst, the observed extent of halo gas would suggest a peak L_{FIR} of ~ 100 times its present value of $L_{\text{FIR}} = 3.5 \times 10^9 L_{\odot}$, equivalent to an estimated SFR of order $50\text{--}100 M_{\odot} \text{ yr}^{-1}$ (using the relations described in § 2). A starburst of this magnitude would have placed NGC 5746 among ultraluminous infrared galaxies (ULIRGs) rather than “normal” starburst (Grimes et al. 2005). The cause of such a powerful starburst occurring within the last few Gyr is not clear, however; ULIRGs seem to be the products of major mergers of gas-rich galaxies (mass ratio less than 3:1; Dasyra et al. 2006), but NGC 5746 is isolated and does not show any immediate evidence for previous violent interactions with other galaxies.

In summary, we cannot entirely rule out a stellar origin for the extraplanar X-ray emission, but comparison to other spirals with and without such emission indicates that the halo of NGC 5746 does not fit well into such a scenario.

6.2. AGN Outflows

Outflows of gas could alternatively be produced by AGN activity. The brightest central X-ray point source inside D_{25} , at $(\alpha, \delta)_{2000} = (14^{\text{h}}44^{\text{m}}56^{\text{s}}.0, 01^{\circ}57'18'')$, exhibits a total of ~ 350 net counts (0.3–5 keV). Fitting a doubly absorbed power-law to its spectrum produces a good fit ($\chi^2_{\nu} = 0.89$), with $\Gamma = 1.38^{+0.29}_{-0.22}$, and $N_{\text{H}} = 7.7^{+3.5}_{-3.4} \times 10^{21} \text{ cm}^{-2}$ for the intrinsic absorption. While this is consistent with a typical AGN spectrum, the absorption-corrected 0.3–5 keV luminosity of $1.9^{+1.2}_{-0.7} \times 10^{40} \text{ erg s}^{-1}$ suggests very moderate activity. Given the distance to NGC 5746, it is furthermore possible that the source in fact remains unresolved in our X-ray data. The *Chandra* spatial resolution corresponds

to a physical extent of $\gtrsim 75$ pc at this distance, so the derived luminosity should probably be viewed as an upper limit. There is also no evidence for any significant nuclear radio source in the VLA data (cf. Fig. 1). Moreover, any associated AGN outflow perpendicular to the disk would be highly collimated, and there is no indication that this is the case (Fig. 1). A 2–7 keV image, in which any AGN should stand out more prominently than in Fig. 1, confirms the lack of spatial substructure in the hard X-ray emission and shows that this emission is confined to the very central regions of the disk. The stellar kinematics in the nuclear region also shows that any central black hole must be of rather modest mass (Bower et al. 1993).

Finally, gas in an AGN outflow would also be unlikely to have attained thermal equilibrium and so would probably not be well described by a thermal plasma model, in contrast to observations. Indeed, AGN outflows in galaxy clusters (where they can be more easily detected due to the influence on the surrounding intra-cluster medium) seem to be associated with bubbles of relativistic non-thermal radio plasma (e.g. Birzan et al. 2004), rather than with soft X-ray emitting material. In fact, these radio bubbles typically coincide with “cavities” in the surrounding intracluster X-ray gas, and in the well-studied case of the Perseus cluster are consistent with containing *no* detectable thermal X-ray gas, even in very deep X-ray observations (J. Sanders, private communication). The detection of an AGN-generated X-ray halo around NGC 5746 in these *Chandra* data would therefore be a major surprise. Hence, as also concluded in Paper I, it seems safe to exclude the possibility that recent or previous AGN activity should be responsible for the extraplanar X-ray emission in this case.

6.3. Accretion of Intergalactic Gas

The only obvious remaining explanation for the X-ray emission around NGC 5746 is the radiative cooling of hot gas residing in an extended gaseous halo which has not been generated by processes in the disk. Since such externally accreted gas is expected to have low metallicities, whereas disk outflows could have (super)solar abundances, a decisive way to test the accretion scenario against an outflow origin for the hot gas would be a robust estimate of the gas metallicity. This could be achieved with deep X-ray spectroscopy, but is unfortunately not feasible with the present data. There are, however, a number of arguments which strengthen the interpretation that the X-ray emission represents externally accreted gas.

(i) The low metallicity derived for the halo gas, $Z \approx 0.1 Z_{\odot}$, indicates an external origin, although, as mentioned, this result could be affected by the Fe bias. Taken at face value, the result is in good agreement with that found for gas presumably accreting onto the Milky Way (Wakker et al. 1999), and also corresponds to the value derived for the low-redshift intergalactic medium (Danforth et al. 2006).

(ii) The temperature of halo gas is consistent with the expected virial temperature of the underlying dark matter halo, suggesting that the gas has been gravitationally heated. This is generally not the case for X-ray gas within (stellar) outflows, which show temperatures that are largely independent of the stellar (e.g.

Rasmussen et al. 2004b or total (see § 7) galactic mass. Of course, the agreement between T_{vir} and the observed temperature for NGC 5746 could be a coincidence, but:

(iii) Not only the temperature, but also the X-ray luminosity, surface brightness profile, and total hot gas mass of the NGC 5746 halo are matched by predictions of cosmological simulations involving infall of hot gas onto spirals (see § 7). Again, a good match between simulations of infall and disk outflows would generally not be expected, and, indeed, is not observed. If the hot gas surrounding NGC 5746 originated within the disk, the agreement with our simulations in § 7 would be a spectacular and, to our knowledge, unique coincidence.

Although a direct confirmation of the accretion scenario would require more sensitive X-ray data, it appears to be the most plausible explanation in light of the above discussion. When interpreted in this way, the extraplanar X-ray emission of NGC 5746 thus represents the first tentative detection of the hot halos of externally accreted gas in which massive spiral galaxies are believed to be embedded. One should note, then, that simulations show such halo gas to display a range of temperatures (albeit a fairly narrow one outside the disk; see § 7), so the model fits of Table 2 should be considered a convenient means of parametrizing the halo X-ray properties rather than a complete description of the physical state of hot halo gas.

6.4. Is the Halo Gas Currently Inflowing?

In the accretion scenario discussed above, halo gas is expected to be actively accreting onto the disk due to the decreased pressure support of the rapidly cooling gas close to the disk. The question of whether the observed gas is really falling in at present naturally bears some connection to the issues discussed above. As mentioned, the mean cooling time at D_{25} is only ≈ 4 Gyr, and any thermal instabilities in the gas would act to locally reduce this value, likely leading to the condensation of clouds of colder material which can accrete onto the disk (Kaufmann et al. 2006; Sommer-Larsen 2006). Therefore, if cooling and the ensuing inflow of halo gas is not counteracted by feedback, the X-ray emitting material should currently be accreting onto the disk. However, although the halo itself may be unlikely to result from SN/AGN activity, it is conceivable that the energy released by such processes is currently preventing halo gas from actually inflowing (see e.g. Binney 2004), either through mechanical $p dV$ work done on this gas or through re-heating of gas which has cooled to $T \lesssim 10^6$ K. Unfortunately, the present data do not allow us to directly assess the validity of this scenario, but some insight can be gained from more indirect arguments. If assuming that the spatial distribution of energy input to the halo roughly matches that of radiative losses from the halo, an upper limit to the energy required to offset cooling and gas infall would simply be the halo luminosity, $L_X \approx 7 \times 10^{39}$ erg s $^{-1}$.

In principle, the mechanical output generated by an AGN could provide this power. Strong radio sources associated with nuclear activity in elliptical galaxies are emerging as prime candidates for retarding and even quenching cooling flows on a variety of scales. This probably occurs via a feedback-driven activity cycle of duration $\sim 10^8$ yr, and could be effective both in

individual ellipticals and in the cores of groups and clusters (e.g. Fabian et al. 2003; Voit & Donahue 2005; Best et al. 2006). However, there is little evidence from Fig. 1 for current or even past strong radio activity in NGC 5746 (i.e. a bright nuclear radio source, radio outflows from the disk, and/or extended radio emission some distance from the disk as a result of previous activity). This suggests that any AGN may currently be in a quiescent phase of its activity cycle, but it also precludes any direct estimate of the energy output of an AGN in its active phase.

Nevertheless, an estimate of the maximum AGN energy output in NGC 5746 may be obtained from the results of Birzan et al. (2004). These authors studied a sample of 18 galaxy systems ranging from rich clusters down to a single elliptical galaxy, in which cavities in the surrounding X-ray gas can be associated with outflows generated by current or past activity of a radio source in the central galaxy. They found a correlation between the radio luminosity of this central source and estimates of the mechanical luminosity $L_{\text{mech}} = W/t$ of the cavities. Here W is the $p dV$ work done by the cavity on the surrounding X-ray gas as it rises buoyantly through this gas, and t is the age of the cavity. Though the derived relation is subject to substantial scatter, it remains useful for providing a rough estimate of the mechanical energy released by the central radio source in NGC 5746 in any active phase. The 1.4 GHz continuum flux of this source of 14.9 mJy (Condon et al. 1998) would correspond to a total radio luminosity of $\sim 1 \times 10^{38}$ erg s $^{-1}$, calculated using the prescription of Birzan et al. (2004) and assuming a spectral index $\alpha = 1$. In turn, the relation derived by Birzan et al. (2004) would then suggest L_{mech} of order 10^{41} erg s $^{-1}$ which could be sufficient to counteract infall.

However, as also noted by Birzan et al. (2004), this estimate could suffer from considerable systematic uncertainties, and it is moreover unclear whether their results are representative of the overall efficiency with which AGN mechanical energy is transferred to its surroundings. For example, the result is based on a sample for which X-ray cavities *can* be detected and which does not include any spiral galaxies. The only safe conclusion, it seems, is that an AGN in an active phase (assuming AGN in isolated spiral galaxies have activity cycles as seen for central cluster galaxies, although there is little support for this assumption at present) could potentially halt cooling and infall of halo gas, but that there is no significant evidence from X-ray or radio data of any ongoing or recent activity of this type. Hence, our observations do not allow a direct test of the hypothesis put forward by Binney (2004), that once a hot gaseous halo has been built up around a galaxy, its gas does not cool but rather remains thermostated at $T \approx T_{\text{vir}}$ due to energy injection from an AGN (and stars). Although significant AGN activity does not seem to be taking place at present in NGC 5746, the existing radio data probably lack the sensitivity to allow an unambiguous test for such activity in the recent past. This is certainly true for the X-ray data, leaving Binney’s hypothesis a viable possibility.

Supernova outflows provide an alternative means of preventing infall of halo gas. While the total SN rate of NGC 5746 of ~ 0.02 yr $^{-1}$ (§ 6.1) is probably insuf-

ficient to blow gas out of the disk, as discussed above, it still corresponds to a mechanical energy release of $\approx 1 \times 10^{42}$ erg s $^{-1}$ for a typical SN output of 10^{51} erg. Simulations suggest that, under normal interstellar conditions, most (~ 90 per cent) of this energy is radiated away (Thornton et al. 1998); in fact, this would be consistent with the diffuse disk luminosity of NGC 5746 if assuming an intrinsic absorption in the disk equal to that derived for the central X-ray point source. Of the remaining energy, a small fraction is expected to thermalize in the interstellar medium of the disk, leaving a mechanical luminosity which could still be an order of magnitude larger than the halo L_X . Although insufficient to blow gas out of the disk and hence entirely inhibit halo gas infall, it will, in particular in combination with any nuclear activity, act to reduce the infall rate and perhaps also reheat some of the already cooled accreting gas, making it at least temporarily unavailable for star formation. In practice, this implies that the derived mass accretion rate \dot{M} of external halo gas must be viewed as an upper limit under the given assumptions.

Future tests, involving deeper X-ray and far-ultraviolet observations, could shed light on these issues. For example, if much of the halo gas is held in place by activity in the disk, one would expect enriched material from the disk to have mixed with halo gas, so a more robust X-ray metallicity constraint would be highly useful. To test if cooling does occur outside the disk, one could look for evidence of a temperature gradient in the halo X-ray gas (although, as discussed in § 7, the absence of a T -gradient outside the disk does not necessarily imply that gas is not cooling rapidly even further in). Finally, one could test whether gas is cooling below X-ray temperatures using *FUSE* observations of OVI at a range of distances from the disk, although the expected low metal content of halo gas may render such observations difficult.

Summarizing, there is no direct observational evidence for any AGN or SN activity at levels sufficient to completely offset cooling and infall of halo gas in NGC 5746, and indirect arguments indicate that the required power for this to occur is not currently available. Consequently, given the derived cooling time of halo gas, some of this gas should currently be accreting onto the disk, acting as a fresh supply of material for continued star formation. If so, the disk of this massive spiral is still being built up at present.

7. COMPARISON TO SIMULATIONS OF GALAXY FORMATION

In the accretion scenario, halo properties can be predicted in detail by cosmological simulations. Hence, it is natural to compare the results obtained for both our galaxies to numerical work. To this end, we have employed cosmological TreeSPH simulations of galaxy formation and evolution in a flat Λ CDM cosmology. The code, described in detail in Sommer-Larsen et al. (2005) and Romeo et al. (2006), incorporates energetic stellar feedback taking the form of starburst-driven galactic winds. With respect to our earlier simulations used by Toft et al. (2002) to predict halo properties (as discussed in § 1 and § 2), the present simulations have been updated to incorporate chemical evolution of the gas, including non-instantaneous recycling, and are evolved in time according to the entropy equation solving scheme

of Springel & Hernquist (2002), rather than being based on the thermal energy equation. The latter improvement provides increased numerical accuracy in lower-resolution regions. In addition, the present simulations have all been run with at least eight times higher mass resolution. The highest resolution runs of individual galaxies, at 512 times the resolution of the simulations described by Toft et al. (2002), feature a total of $\sim 2 \times 10^5$ gas and $\sim 1.5 \times 10^5$ dark matter particles inside $(100 \text{ kpc})^3$, a gas mass resolution of $1.2 \times 10^4 M_\odot$, and a corresponding gravitational softening length of $\sim 130 \text{ pc}$.

Although the simulations include stellar feedback, optionally enhanced to mimic AGN outflows, starburst-driven winds are only invoked at early times ($z \gtrsim 4-5$), in order to solve the angular momentum problem, the missing satellites problem, and possibly other problems related to the cold dark matter scenario (see, e.g., Sommer-Larsen et al. 2003). At $z \lesssim 4$, the SN II feedback is quite moderate in our simulations; for a typical $v_c = 220 \text{ km s}^{-1}$ disk galaxy, the star formation rate at $z = 0$ is $\sim 0.5 - 1 M_\odot \text{ yr}^{-1}$, similar to the modest star formation rate of the Milky Way disk. The feedback of the individual star particles in the simulations is furthermore spatially and temporally uncorrelated, implying that starburst winds do not easily develop at low redshift (see also Dahlem et al. 2006). Hence, a comparison between the simulations and our two relatively quiescent galaxies seems justified.

It is worth emphasizing that the feedback strength in the simulations is calibrated to reproduce the *optical* properties of observed galaxies, but that the X-ray emission is predicted without any additional adjustable parameters. We find that neglecting feedback in the simulations tends to decrease the present-day halo X-ray luminosity, because less feedback implies that hot halo gas cools out faster over cosmic time, leaving less hot gas in the halo at $z = 0$ (the situation is qualitatively similar to the difference between assuming fixed, primordial metallicity and $Z = 0.3 Z_\odot$ for the halo gas in the simulations, as discussed by Rasmussen et al. 2004a). We note in passing that this also implies that the predictions of semi-analytical models of galaxy formation (which tend to over-predict halo L_X with respect to observations) and those of our simulations cannot be reconciled simply by neglecting feedback in the simulations.

For the calculation of X-ray properties of the simulated galaxies, we follow the procedure outlined by Toft et al. (2002), except that the increased numerical resolution of the present simulations allows us to bypass the smoothing over the individual gas particles in the simulations. All simulation results have been derived inside a region corresponding to the adopted NGC 5746 halo aperture (region B/E of Table 2). A few comparisons between NGC 5746 and results from these simulations were performed in Paper I, showing the simulation predictions to be in good agreement with the observed X-ray surface brightness profile and integrated halo L_X . Below we will elaborate on these and other simulation results, present additional comparisons to observed galaxies, and discuss the implications for models for the formation of spiral galaxies.

7.1. X-ray Luminosity, Temperature, and Surface Brightness

Figure 6a displays results based on our recent simulations described above, run at 8, 64, and 512 times the resolution of the Toft et al. (2002) simulations. Of the new simulations, the one producing the galaxy with $v_c \approx 226 \text{ km s}^{-1}$ assumes a cosmic baryon fraction $f_b = 0.10$, whereas those of higher- v_c galaxies assume $f_b = 0.15$. Also shown are results for a subsample of the simulated galaxies of Toft et al. (2002). These were all formed in simulations assuming either a Λ CDM or Λ WDM cosmology of $\Omega_m = 0.3$ and $\Omega_\Lambda = 0.7$, $f_b = 0.10$, and a (fixed) primordial chemical gas composition. The X-ray luminosity of these simulated galaxies have been corrected for the error described in Rasmussen et al. (2004a). The correlation of L_X with v_c is seen to display notable scatter, most of which is related to intrinsic differences in the accretion history of the galaxies (Toft et al. 2002). In general, there seems to be good agreement between the two simulation samples. While numerical resolution effects seem to play a limited role in establishing the predicted L_X - v_c trend or its scatter, there is some indication that increased resolution tends to lower the predicted halo luminosity by a small amount.

Figure 6a also displays the derived constraints on the halo luminosities of NGC 5170 and NGC 5746, and has been updated from Paper I to show the additional constraints obtained for the extraplanar emission seen around other spirals, i.e. the comparison sample also plotted in Fig. 5. In these cases, the halo luminosities have not necessarily been derived within the same aperture as adopted for NGC 5746 and our simulated galaxies. For example, the results of Strickland et al. (2004) were all derived at a distance $|z| > 2 \text{ kpc}$ from the disk midplane. If instead adopting this aperture, the increase in L_X predicted for our simulated galaxies is at the 10–40 per cent level, with no systematic dependence on v_c . We expect similar corrections for the apertures used for the other observed samples. These changes are relatively small, being within the scatter seen for the simulated galaxies and the estimated uncertainties in L_X for NGC 5746. We have therefore chosen not to correct for this effect in Fig. 6a, as the overall conclusions will clearly remain unaffected by such a change. We also show the strongest constraint resulting from the study of Benson et al. (2000), the 3σ upper limit to the halo L_X of NGC 2841, here converted to the 0.3–2 keV band assuming a *mekal* thermal plasma of $T \approx 0.4 \text{ keV}$ based on the (T, v_c) plot of Toft et al. (2002). This result was originally derived within a 5–18 arcmin annulus around the galaxy, so the value has been corrected to the NGC 5746 aperture on the basis of the mean difference in L_X between the two apertures as predicted for the galaxies in our new simulations (amounting to a factor ~ 3 increase in L_X). As can be seen from the figure, the simulation results generally appear to be in excellent agreement with those of our observed galaxies. In particular, the theoretical models provide a good match to the derived halo luminosity of NGC 5746, and their predictions can easily be accommodated by the observational results for the (presumably mainly feedback-generated) hot halos seen in other studies.

It is worth noting that the emission-weighted mean metallicity of the X-ray gas in these simulations is very low, of order $10^{-3} Z_\odot$, predicting the inflowing gas to be essentially primordial in composition. Those simu-

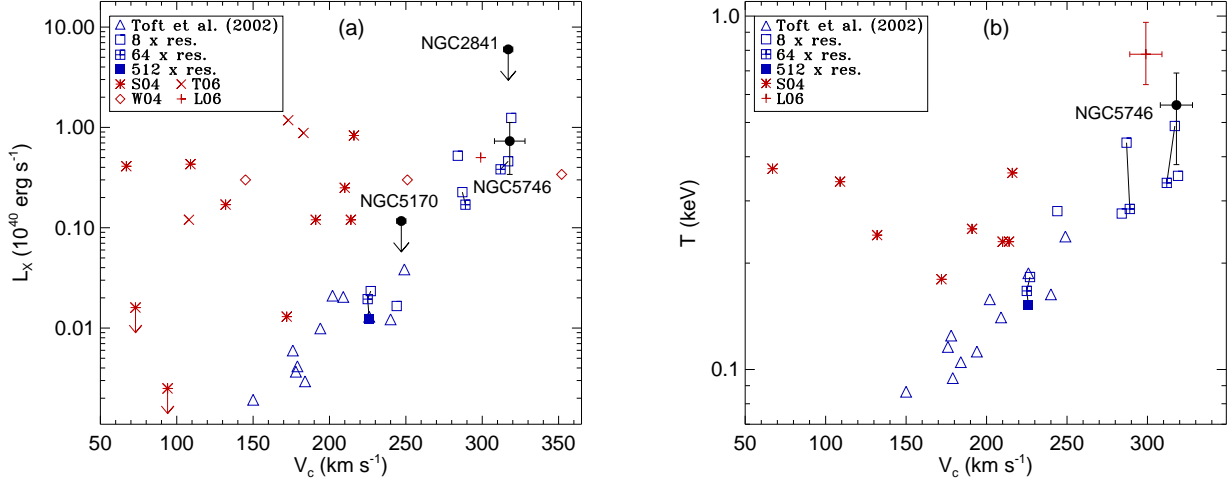


FIG. 6.— (a) X-ray luminosity and (b) emission-weighted hot halo temperature versus v_c for the simulated galaxies of Toft et al. (2002; triangles) and for those in our new simulations (squares), all calculated assuming the NGC 5746 halo aperture. Simulations of the same galaxy run at different resolutions are connected by a line. Also shown are the available observational results, with symbols as in Fig. 5.

lations of Toft et al. (2002) that assume a fixed metallicity of $0.3 Z_\odot$ would, for a given v_c , predict present-day luminosities 3–4 times *lower* than those shown in Fig. 6a (cf. the above discussion). This would still leave NGC 5746 within the dispersion in the predicted L_X – v_c trend, but the agreement would be considerably less convincing. This may indicate that any hot gas accreted by spirals today is nearly pristine; a similar result emerges when comparing simulations of galaxies at high redshift to observational constraints on the redshift evolution of the *integrated* X-ray luminosity of normal spirals (Rasmussen et al. 2004a).

Figure 6b shows the temperature of hot halo gas versus v_c . Despite the large variation in accretion history among the simulated galaxies, the simulations predict a remarkably tight correlation between the two quantities. The prediction is consistent with the value derived for NGC 5746 and with the expected virial temperature of its dark matter halo, $T_{\text{vir}} \approx 0.3$ keV. The result for NGC 5746 is larger than T_{vir} but, at a level of 1.4σ , not significantly so. A plausible explanation could be related to the fact that the hot halo spectrum of NGC 5746 is dominated by emission close to the disk, and, as demonstrated below, the simulations predict that the temperature of hot halo gas rises slightly above the virial temperature close to the disk. We note that a halo gas temperature slightly exceeding the virial temperature of the dark matter is also a generic feature of the hot halo models considered by Fukugita & Peebles (2006).

For comparison to our simulations, the corresponding data for the Strickland et al. (2004) sample and the Li et al. (2006) result have once again been overplotted in Figure 6b. Emission-weighted halo temperatures have not been published for the samples of Wang (2004) or Tüllmann et al. (2006a), so these galaxies are not included in this diagram. The lack of a systematic trend (in both L_X and T) with v_c , and hence galactic mass, within these samples is another argument against a gravitational origin for their extraplanar emission. This interpretation gains support from the fact that the hot halo temperatures of these galaxies consistently exceed the virial tem-

peratures expected from the circular velocity of the disk and are furthermore invariant with respect to L_X over four orders of magnitude in SFR (Grimes et al. 2005). Gas is almost certainly outflowing rather than infalling in these cases.

It is also worth emphasizing that our non-detection of any hot halo surrounding NGC 5170 is consistent with the simulation results, assuming its luminosity and temperature within the relevant aperture can be reliably predicted from Fig. 6. For an estimated halo luminosity and temperature of $L_X \approx 10^{39}$ erg s $^{-1}$ and $T \approx 0.2$ keV, respectively, we predict only ~ 15 net halo counts in 0.3–2 keV, well within the Poisson noise of the background. This supports our use of the NGC 5170 data in § 4 as a testbed for our analysis procedure.

In Fig. 7a, we plot surface brightness profiles of the simulated galaxies, extracted within the same physical aperture as for NGC 5746, and co-added on either side of the disk as in Fig. 2. In order to include the result for NGC 5746 in this diagram, the background subtracted count rates for NGC 5746 were converted into unabsorbed fluxes assuming a *mekal* plasma of the best-fitting halo parameters (Table 2) and the Galactic value of N_{H} . For this conversion, a 30 per cent systematic uncertainty was added in quadrature to the statistical errors shown in Fig. 2, on the basis of the derived errors on spectral parameters. The simulations of galaxies with $v_c \approx 300$ km s $^{-1}$ seem to produce results consistent with the observed NGC 5746 profile for the adopted aperture. To give an appreciation of the effects of numerical resolution, results for the $v_c \approx 226$ km s $^{-1}$ simulated galaxy also shown in Fig. 6 are overplotted. There is some indication that the predicted profile flattens for higher resolutions, but not to an extent that would compromise the above conclusion. Furthermore, simulation results for the innermost bin cannot be compared directly to observations, because much of the halo emission in this region would be absorbed by neutral gas in the disk of an edge-on galaxy and would moreover suffer contamination from unrelated emission associated with hot gas in the disk.

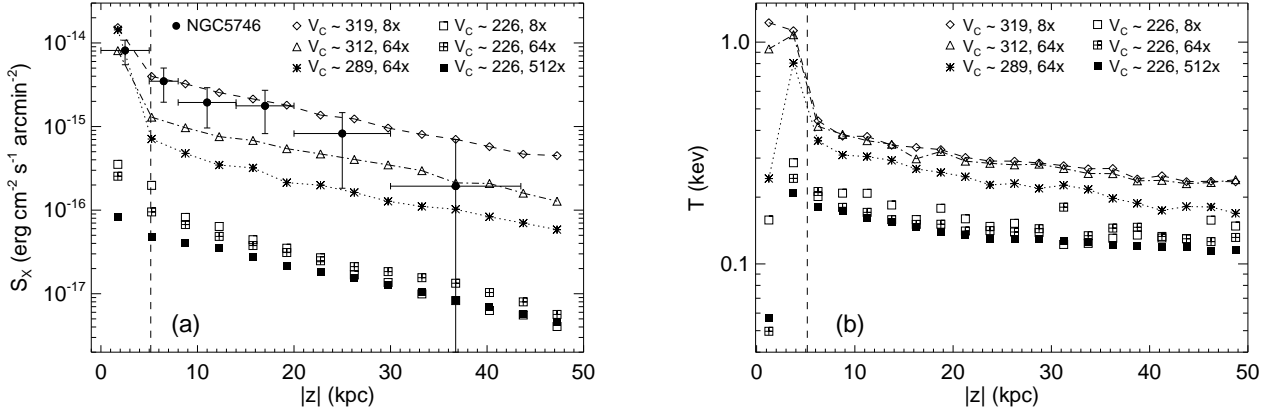


FIG. 7.— (a) Derived surface brightness profile for NGC 5746 along with those of simulated galaxies in the relevant mass range, all computed inside a region corresponding to region A of Fig. 1. Dashed vertical line marks the extent of the D_{25} minor axis of NGC 5746. (b) The corresponding emission-weighted temperature profiles of the simulated galaxies, with symbols and lines as in the left figure.

The hot gas temperature of the simulated galaxies, plotted in Fig. 7b, is seen to occupy a range of values, which is, however, reasonably narrow outside the ‘disk’. Well outside the disk, the predicted halo temperature is in excellent agreement with the virial temperature expected for the simulated galaxies (i.e. $T \approx 0.3$ keV for a galaxy with $v_c \approx 300$ km s⁻¹). Closer to the disk, T increases gently and then rises steeply in the innermost ~ 5 kpc above the disk midplane, followed by a strong decline as the gas eventually reaches a density which enforces rapid cool-out onto the disk. The reasonably uniform temperature distribution predicted outside the disk suggests that our usage of a single-temperature model for the description of the halo spectrum is supported on a physical basis, and that the Fe bias may not be significantly affecting our metallicity measurement. However, it also indicates that, although gas is cooling rapidly in the central halo regions, the gas outside the disk could be near-isothermal. One implication is that X-ray observations of extraplanar gas around spirals may not be able to directly test whether this gas is indeed cooling out of the X-ray phase, as much of the cooling occurs very close to the disk where contamination from other X-ray sources, diffuse and point-like, could be substantial.

7.2. Hot Gas Mass and Accretion Rates

The amount of hot X-ray gas surrounding the simulated galaxies depends not only on the mass of each galaxy’s dark matter halo but also on the detailed accretion history of this halo. Accretion histories can be highly disparate even for isolated galaxies of comparable mass (e.g. van den Bosch 2002; Rasmussen et al. 2004a). Any relation between the mass M_{gas} of hot halo gas and v_c (or L_X and v_c) is thus expected to display considerable intrinsic scatter, as indeed evidenced by Fig. 8a. In this plot we show the gas mass of the simulated galaxies inside the volume assumed in the corresponding calculation for NGC 5746 (§ 5.1), i.e. excluding the volume covered by D_{25} of NGC 5746 out to 45 kpc from the disk center along the line of sight. Given that the simulations also include cold, non-X-ray emitting gas around the galaxies and that M_{gas} is not an X-ray emission-weighted quan-

tity, a low-temperature cut of $T = 0.1$ keV has been imposed on the simulated galaxies in order to provide a fair comparison to observations. This temperature is probably the lowest one at which gas can be reliably detected by *Chandra* or *ROSAT* (see, for example, the discussion in Rasmussen et al. 2004b). For completeness, we also show the mean effect of this T -cut for four intervals in v_c . Simulation results are again seen to be in good agreement with the observational constraints.

Fig. 8b shows the mass deposition rate $\dot{M} \approx M_{\text{gas}}/t_{\text{cool}}$ of hot gas (which for all galaxies should be viewed as an upper limit, cf. § 6.4). Again, a temperature cut at $T = 0.1$ keV has been imposed on the simulations, but \dot{M} has otherwise been estimated in the same manner as for the observed galaxies. The figure reveals substantial scatter at any given v_c and no clear systematic variation with this quantity. The cool-out rate of NGC 5746 lies at the low end of the range predicted by simulations, but there is also an indication that numerical resolution effects might play a role, in the sense that increased resolution tends to lower \dot{M} within the adopted aperture.

The actual mass of hot halo gas which is cooling out around NGC 5746 would include any gas cooling within D_{25} . In the present data, emission from such gas cannot be separated from diffuse disk emission resulting from stellar activity. Based on the simulated galaxies covering the relevant mass range ($v_c > 255$ km s⁻¹), we estimate that accounting for cooling inside the disk region would raise \dot{M} by a factor $\xi \sim 5$ –10, if assuming similar levels of feedback in the simulated galaxies as for NGC 5746. For the derived value of $\langle \dot{M} \rangle$ (Table 3), this would imply a total cool-out rate of ~ 1 –2 M_\odot yr⁻¹, in good agreement with the *IRAS*-based estimate of the disk star formation rate (SFR) of NGC 5746, 0.8 ± 0.2 M_\odot yr⁻¹ (§ 2). While only an indicative result, this suggests that the galaxy is currently forming stars at a rate corresponding to that at which gas can be supplied for this process from the hot halo. For NGC 5170, the derived limit to the hot gas cooling rate, $\dot{M}_{\text{cool}} < 0.2$ M_\odot yr⁻¹, is a somewhat more model-dependent result than that of NGC 5746, as it is based on an assumed value of the halo temperature. The

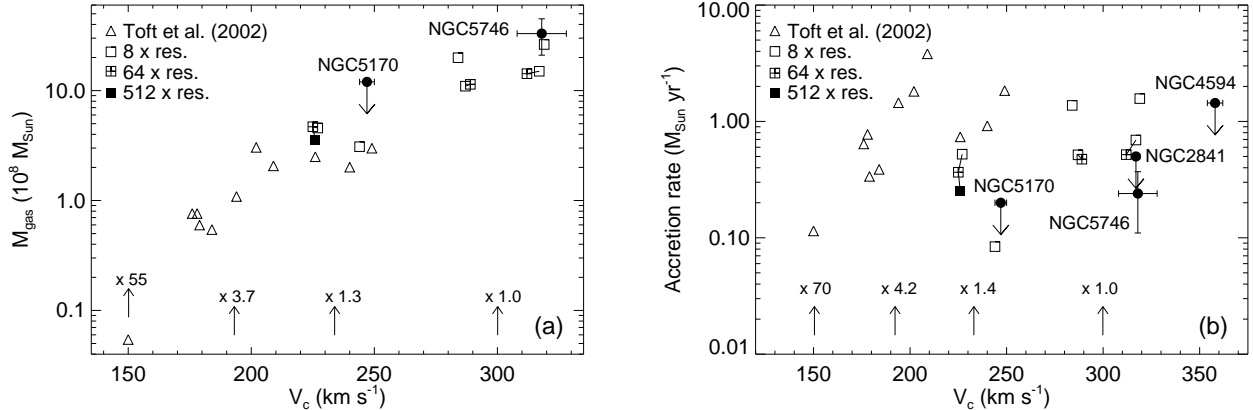


FIG. 8.— (a) Mass of hot ($T \geq 0.1$ keV) gas as a function of v_c within the NGC 5746 halo aperture. (b) The corresponding hot gas accretion rate, $\dot{M} \sim M_{\text{gas}}/t_{\text{cool}}$. Also shown are the upper limits estimated by Benson et al. (2000) for NGC 2841 and NGC 4594 (the ‘Sombrero’ galaxy). Annotations at upward arrows give the mean factor of increase had all gas hotter than 10^5 K in the simulations (within the aperture) been included in the estimate of M_{gas} . The numbers apply to the intervals $v_c < 160 \text{ km s}^{-1}$, $170 < v_c < 210 \text{ km s}^{-1}$, $210 < v_c < 255 \text{ km s}^{-1}$, and $v_c > 255 \text{ km s}^{-1}$.

derived limit is nonetheless consistent with the disk SFR estimate of $0.3 \pm 0.1 M_{\odot} \text{ yr}^{-1}$, even without accounting for the gas cooling out within the optical disk.

Can the disk of NGC 5746 have been built up by the accretion of hot halo gas over cosmic time? Since stars are dominating the mass of visible matter in the disks of spiral galaxies, the total baryonic disk mass of NGC 5746 can be estimated from its K - and B -band luminosities using the prescription of Mannucci et al. (2005). This yields a baryonic mass of $3.0 \times 10^{11} M_{\odot}$. In order to estimate the total mass M_{acc} of hot gas accreted by NGC 5746 since a given redshift, we can extrapolate the present accretion rate by assuming

$$\log \dot{M}(z) \approx 0.6z + C. \quad (2)$$

This follows the redshift evolution found by Rasmussen et al. (2004a) for the accretion of hot ($T \gtrsim 3 \times 10^5$ K) gas by spirals formed in cosmological simulations. The relation was derived for simulated galaxies with present-day masses similar to that of the Milky Way, and applies to the redshift interval $z = 0 - 2$, prior to which the galactic disks themselves are not well-defined in the simulations. For NGC 5746, we have an upper limit (for $\xi = 10$) of $\dot{M}(z = 0) \lesssim 4 M_{\odot} \text{ yr}^{-1}$. Choosing the constant C such as to match this present upper limit, one then arrives at a corresponding upper limit to the total mass of hot gas accreted by NGC 5746 since $z = 2$ of $M_{\text{acc}} \lesssim 1.2 \times 10^{11} M_{\odot}$, which is somewhat below, yet comparable to, the present baryonic mass in the disk of NGC 5746.

However, this extrapolation is based on simulation results for Milky Way-sized galaxies and could be subject to considerable systematic uncertainty. On the one hand, some accretion would have taken place before $z = 2$, during a period in which the star formation activity and the growth of a central supermassive black hole would have been much more vigorous and could have counteracted gas accretion to a significant extent. On the other hand, given its deeper gravitational potential, it is conceivable that accretion was initiated earlier for NGC 5746 than

for typical Milky Way-like galaxies (on which Eq. 2 is based) and would have been more dramatic at high redshifts than for such galaxies. A more pronounced redshift evolution of the cooling rate than the one adopted here can, in fact, be accommodated within the constraints on the redshift evolution of the integrated X-ray luminosity of spirals derived from *Chandra* Deep Field data (Rasmussen et al. 2004a).

Consequently, the current observational evidence is consistent with the notion that a sizable fraction of the disk mass of NGC 5746 has been formed by the accretion of hot X-ray emitting halo gas. Although this is in encouraging agreement with recent cosmological models for the formation of massive spirals, we acknowledge that this conclusion is clearly a model-dependent result. Moreover, Equation (2) does not account for the accretion of *cold*, non-X-ray emitting gas, the addition of which would likely bring the extrapolation into even better agreement with the observed disk mass. It is therefore clearly premature to exclude the possibility that a significant fraction of the infalling gas around NGC 5746 was either never or only briefly heated to X-ray temperatures. In that case, accretion may, at least partly, have proceeded much as in the ‘cold mode’ accretion scenarios originally suggested by Binney (1977) and later followed up by various authors (Birnboim & Dekel 2003; Binney 2004; Kereš et al. 2005; Sommer-Larsen 2005).

8. SUMMARY

Our *Chandra* data of the two massive edge-on disk galaxies NGC 5170 and NGC 5746 have revealed a 5σ detection of extraplanar X-ray emission around the more massive NGC 5746, extending to at least ~ 20 kpc above the disk. No detection is found around NGC 5170 using the same analysis methods, which rules out the possibility that the NGC 5746 result is due to instrumental artefacts or details of our analysis. Both galaxies are isolated and show no signs of significant nuclear or star formation activity. For NGC 5746, this is also confirmed from our $H\alpha$ imaging of this galaxy, leading to the conclusion that

the diffuse X-ray emission surrounding NGC 5746 is best explained as the signature of externally accreted gas cooling radiatively in an extended hot halo. The spectrum of this hot halo gas is well described by a thermal plasma model of temperature ~ 0.5 keV, with an indication that the gas metallicity is very low, $Z \lesssim 0.1 Z_{\odot}$, although deeper data would be needed to confirm this. The total 0.3–2 keV luminosity of the hot halo is $\sim 7 \times 10^{39}$ erg s $^{-1}$, while the corresponding 3σ upper limit for the NGC 5170 halo is $\sim 3 \times 10^{39}$ erg s $^{-1}$.

We have performed a detailed comparison of the derived constraints on halo X-ray properties of both galaxies to cosmological simulations of galaxy formation and evolution which predict the existence of such a halo. Very good overall agreement is found for the case of NGC 5746, supporting our interpretation that the detected extraplanar X-ray emission around this galaxy reflects the cooling of accreted hot gas rather than being related to ongoing processes in the disk (such as supernova-driven outflows of gas). The weaker limits obtained for the non-detected halo around NGC 5170 are also easily consistent with simulation predictions. We also note that the results obtained for all other galaxies with detected extraplanar emission are consistent with our simulations.

Although the presence of accreted hot gas halos around spiral galaxies has been hypothesized for almost 50 years, the observed X-ray emission surrounding NGC 5746 seems to be the first, albeit tentative, detection of such a halo. This lends support to one of the outstanding issues in many models of disk galaxy formation, namely the assumption that extended reservoirs of accreted hot gas exist around isolated high-mass disk galaxies, potentially supplying material for the formation and growth of the baryonic component of such galaxies even to the present day. Moreover, it indicates that the "missing" galactic baryons are, in fact, not missing, but mostly are constituted by hot halo gas, as discussed by Sommer-Larsen (2006). However, we stress that a decisive test of the accretion hypothesis for the gas surrounding NGC 5746 would require more sensitive X-ray data; in particular, deep X-ray spectroscopy would enable a robust metallicity estimate for the halo gas, helping to distinguish

between infall and outflow models.

The estimated cooling rate of hot halo gas around NGC 5746 is found to be consistent with predictions from simulations and with the current star formation rate in the disk. We have estimated the total mass of hot gas accreted by this system over cosmic time, indicating that a significant fraction of the current disk mass can have been formed through the infall of hot gas. This is consistent with many semi-analytical models of the formation of massive spirals. It remains a viable possibility, however, that a substantial fraction of the present material in the disk has been accreted as cold ($T \lesssim 10^5$ K), non-X-ray emitting gas (such as the high-velocity clouds seen around the Milky Way). We find that the present data do not allow for a direct quantification of the relative importance of 'cold' and 'hot' accretion over the lifetime of the galaxy. More sensitive X-ray observations of NGC 5746 and similar galaxies, coupled with results of dedicated galaxy formation simulations, would be needed to settle this issue.

This work has made use of the HyperLeda and NASA/IPAC (NED) extragalactic databases, and the Two Micron All Sky Survey database. JR and KP acknowledge support from the Instrument Center for Danish Astrophysics (IDA) during the initiation of this work. JR also acknowledges the support of the European Community through a Marie Curie Intra-European Fellowship. JSL acknowledges support from the Villum Kann Rasmussen Foundation and from Dark Cosmology Centre. ST and LFO acknowledge support from the Danish Natural Sciences Research Council. AJB acknowledges support from a Royal Society University Research Fellowship and from the Gordon & Betty Moore Foundation. RGB acknowledges the support of a PPARC Senior Fellowship. We gratefully acknowledge abundant access to the computing facilities provided by the Danish Centre for Scientific Computing (DCSC), with which all computations reported in this paper were performed. Dark Cosmology Centre is funded by the Danish National Research Foundation.

REFERENCES

- Anders, E., & Grevesse, N. 1989, *Geochim. Cosmochim. Acta*, 53, 197
- Arnaud, M., et al. 2002, *A&A*, 390, 27
- Balogh, M. L., Pearce, F. R., Bower, R. G., & Kay, S. T. 2001, *MNRAS*, 326, 1228
- Benson, A. J., Bower, R. G., Frenk, C. S., & White, S. D. M. 2000, *MNRAS*, 314, 557
- Bertin, E., & Arnouts, S. 1996, *A&AS*, 117, 393
- Best, P. N., Kaiser, C. R., Heckman, T. M., & Kauffmann, G. 2006, *MNRAS*, 368, L67
- Binney, J. 1977, *ApJ*, 215, 483
- Binney, J. 2004, *MNRAS*, 347, 1093
- Birnboim, Y., & Dekel, A. 2003, *MNRAS*, 345, 349
- Birzan, L., Rafferty, D. A., McNamara, B. R., Wise, M. W., & Nulsen, P. E. J. 2004, *ApJ*, 607, 800
- Block, D. L., Bournaud, F., Combes, F., Puerari, I., & Buta, R. 2002, *A&A*, 394, L35
- Bournaud, F., & Combes, F. 2002, *A&A*, 392, 83
- Bournaud, F., Combes, F., Jog, C. J., & Puerari, I. 2005, *A&A*, 438, 507
- Bower, G. A., Richstone, D. O., Bothun, G. D., & Heckman, T. M. 1993, *ApJ*, 402, 76
- Buote, D. A. 2000, *MNRAS*, 311, 176
- Casuso, E., & Beckman, J. E. 2004, *A&A*, 419, 181
- Cen, R., & Ostriker, J. P. 1999, *ApJ*, 514, 1
- Cole, S., Lacey, C. G., Baugh, C. M., & Frenk, C. S. 2000, *MNRAS*, 319, 168
- Condon, J. J., & Broderick, J. J. 1986, *AJ*, 92, 94
- Condon, J. J., Anderson, M. L., & Helou, G. 1991, *ApJ*, 376, 95
- Condon, J. J., Cotton, W. D., Greisen, E. W., Yin, Q. F., Perley, R. A., Taylor, G. B., & Broderick, J. J. 1998, *AJ*, 115, 1693
- Dahlem, M., Lisenfeld, U., & Rossa, J. 2006, *A&A*, 457, 121
- Danforth, C. W., Shull, J. M., Rosenberg, J. L., & Stocke, J. T. 2006, *ApJ*, 640, 716
- Dasyra, K. M., et al. 2006, *ApJ*, 638, 745
- Davé, R., et al. 2001, *ApJ*, 552, 473
- Ebeling, H., White, D. A., & Rangarajan, F. V. N. 2006, *MNRAS*, 368, 65
- Ehle, M. 2004, in *ASP Conf. Ser.* 331, *Extra-Planar Gas*, ed. R. Braun (San Francisco: ASP), 337
- Fabian, A. C., Sanders, J. S., Allen, S. W., Crawford, C. S., Iwasawa, K., Johnstone, R. M., Schmidt, R. W., & Taylor, G. B. 2003, *MNRAS*, 344, L43
- Fraternali, F., & Binney, J. J. 2006, *MNRAS*, 366, 449
- Fukugita, M., & Peebles, P. J. E. 2006, *ApJ*, 639, 590
- Gilfanov, M. 2004, *MNRAS*, 349, 146
- Governato, F., et al. 2004, *ApJ*, 607, 688
- Grimes, J. P., Heckman, T., Strickland, D., & Ptak, A. 2005, *ApJ*, 628, 187
- Hatton, S., Devriendt, J. E. G., Ninin, S., Bouchet, F. R., Guiderdoni, B., & Vibert, D. 2003, *MNRAS*, 343, 75
- Kauffmann, G., White, S. D. M., & Guiderdoni, B. 1993, *MNRAS*, 264, 201

- Kaufmann, T., Mayer, L., Wadsley, J., Stadel, J., & Moore, B. 2006, *MNRAS*, 370, 1612
- Kennicutt, R. C., Jr. 1998, *ApJ*, 498, 541
- Kereš, D., Katz, N., Weinberg, D. H., & Davé, R. 2005, *MNRAS*, 363, 2
- Kuntz, K. D., & Snowden, S. L. 2000, *ApJ*, 543, 195
- Kregel, M., van der Kruit, P. C., & de Blok, W. J. G. 2004, *MNRAS*, 352, 768
- Li, Z., Wang, Q. D., Irwin, J. A., & Chaves, T. 2006, *MNRAS*, 371, 147
- Mac Low, M., & McCray, R. 1988, *ApJ*, 324, 776
- Mannucci, F., della Valle, M., Panagia, N., Cappellaro, E., Cresci, G., Maiolino, R., Petrosian, A., & Turatto, M. 2005, *A&A*, 433, 807
- Moshir, M., et al. 1990, *IRAS Faint Source Catalogue*, version 2.0 (1990)
- Moore, B., & Davis, M. 1994, *MNRAS*, 270, 209
- Nicastro, F., et al. 2005, *Nature*, 433, 495
- Nilsson, K. K., Fynbo, J. P. U., Møller, P., Sommer-Larsen, J., & Ledoux, C. 2006, *A&A*, 452, L23
- O'Sullivan, E., Forbes, D. A., & Ponman, T. J. 2001, *MNRAS*, 328, 461
- O'Sullivan, E., & Ponman, T. J. 2004, *MNRAS*, 349, 535
- O'Sullivan, E., Ponman, T. J., & Collins, R. S. 2003, *MNRAS*, 340, 1375
- Pagel, B. E. J. 1997, *Nucleosynthesis and chemical evolution of galaxies* (Cambridge: Cambridge University Press)
- Pedersen, K., Rasmussen, J., Sommer-Larsen, J., Toft, S., Benson, A., & Bower, R. G. 2006, *New Astronomy*, 11, 465 (Paper I)
- Pietz, J., Kerp, J., Kalberla, P. M. W., Burton, W. B., Hartmann, D., & Mebold, U. 1998, *A&A*, 332, 55
- Quilis, V., & Moore, B. 2001, *ApJ*, 555, L95
- Rasmussen, J., Sommer-Larsen, J., Toft, S., & Pedersen, K. 2004a, *MNRAS*, 349, 255
- Rasmussen, J., Stevens, I. R., & Ponman, T. J. 2004b, *MNRAS*, 354, 259
- Rasmussen, J., Ponman, T. J., & Mulchaey, J. S. 2006, *MNRAS*, 370, 453
- Read, A. M., & Ponman, T. J. 2001, *MNRAS*, 328, 127
- Read, A. M., Ponman, T. J., & Strickland, D. K. 1997, *MNRAS*, 286, 626
- Rice, W., Lonsdale, C. J., Soifer, B. T., Neugebauer, G., Koplan, E. L., Lloyd, L. A., de Jong, T., & Habing, H. J. 1988, *ApJS*, 68, 91
- Rocha-Pinto, H. J., & Maciel, W. J. 1996, *MNRAS*, 279, 447
- Romeo, A. D., Sommer-Larsen, J., Portinari, L., & Antonuccio-Delogu, V. 2006, *MNRAS*, 371, 548
- Rossa, J., & Dettmar, R.-J. 2000, *A&A*, 359, 433
- Rossa, J., Dettmar, R.-J., Walterbos, R. A. M., & Norman, C. A. 2004, *AJ*, 128, 674
- Sanders, D. B., & Mirabel, I. F. 1996, *ARA&A*, 34, 749
- Sanders, D. B., Mazzarella, J. M., Kim, D.-C., Surace, J. A., & Soifer, B. T. 2003, *AJ*, 126, 1607
- Savage, B. D., Lehner, N., Wakker, B. P., Sembach, K. R., & Tripp, T. M. 2005, *ApJ*, 626, 776
- Sembach, K. R., et al. 2003, *ApJS*, 146, 165
- Shen, J., & Sellwood, J. A. 2006, *MNRAS*, 370, 2
- Soltan, A. M. 2006, *astro-ph/0604465*
- Somerville, R. S., & Primack, J. R. 1999, *MNRAS*, 310, 1087
- Sommer-Larsen, J., & Dolgov, A. 2001, *ApJ*, 551, 608
- Sommer-Larsen, J., Götz, M., & Portinari, L. 2003, *ApJ*, 596, 47
- Sommer-Larsen, J. 2005, to appear in the proceedings of "Island Universes: Structure and Evolution of Disk Galaxies", ed. R. de Jong (Springer: Dordrecht) (*astro-ph/0512485*)
- Sommer-Larsen, J. 2006, *ApJ*, 644, L1
- Sommer-Larsen, J., Romeo, A., & Portinari, L. 2005, *MNRAS*, 357, 478
- Spitzer, L., Jr. 1956, *ApJ*, 124, 20
- Springel, V., & Hernquist, L. 2002, *MNRAS*, 333, 649
- Stark, A. A., Gammie, C. F., Wilson, R. W., Bally, J., Linke, R. A., Heiles, C., & Hurwitz, M. 1992, *ApJS*, 79, 77
- Strickland, D. K., & Stevens, I. R. 2000, *MNRAS*, 314, 511
- Strickland, D. K., Heckman, T. M., Colbert, E. J. M., Hoopes, C. G., & Weaver, K. A. 2004, *ApJS*, 151, 193
- Summers, L. K., Stevens, I. R., Strickland, D. K., & Heckman, T. M. 2003, *MNRAS*, 342, 690
- Sutherland, R. S., & Dopita, M. A. 1993, *ApJS*, 88, 253
- Temple, R. F., Raychaudhury, S., & Stevens, I. R. 2005, *MNRAS*, 362, 581
- Thornton, K., Gaudlitz, M., Janka, H.-T., & Steinmetz, M. 1998, *ApJ*, 500, 95
- Toft, S., Rasmussen, J., Sommer-Larsen, J., & Pedersen, K. 2002, *MNRAS*, 335, 799
- Tripp, T. M., Savage, B. D., & Jenkins, E. B. 2000, *ApJ*, 534, L1
- Tully, R. B. 1988, *Nearby Galaxies Catalog* (Cambridge: Cambridge University Press)
- Tüllmann, R., Pietsch, W., Rossa, J., Breitschwerdt, D., & Dettmar, R.-J., 2006a, *A&A*, 448, 43
- Tüllmann, R., Breitschwerdt, D., Rossa, J., Pietsch, W., & Dettmar, R.-J. 2006, *A&A*, 457, 779
- van den Bosch, F. C. 2002, *MNRAS*, 331, 98
- van der Hulst, T., & Sancisi, R. 2004, in *ASP Conf. Ser. 331, Extra-Planar Gas*, ed. R. Braun (San Francisco: ASP), 139
- van Kampen, E., Jimenez, R., & Peacock, J. A. 1999, *MNRAS*, 310, 43
- Voit, G. M., & Donahue, M. 2005, *ApJ*, 634, 955
- Wakker, B. P., et al. 1999, *Nature*, 402, 388
- Wang, Q. D. 2004, in *ASP Conf. Ser. 331, Extra-Planar Gas*, ed. R. Braun (San Francisco: ASP), 329
- Wang, Q. D., Chaves, T., & Irwin, J. A. 2003, *ApJ*, 598, 969
- Wang, Q. D., Immler, S., Walterbos, R., Lauroesch, J. T., & Breitschwerdt, D. 2001, *ApJ*, 555, L99
- White, S. D. M., & Frenk, C. S. 1991, *ApJ*, 379, 52
- White, S. D. M., & Rees, M. J. 1978, *MNRAS*, 183, 341
- Wolfe, M. G., McKee, C. F., Hollenbach, D., & Tielens, A. G. G. M. 1995, *ApJ*, 453, 673